NUCLEIC ACID THERAPEUTICS
Volume 23, Number 4, 2013

DOI: 10.1089/nat.2013.0416

Long Double-Stranded Multiplex siRNAs for Dual Genes Silencing

Wei Peng,[1,2] Jianxin Chen,[1] Yinchao Qin,[1] Zhenjun Yang,[2] and York Yuanyuan Zhu[1]

Simultaneous suppression of multiple oncogenes is an attractive strategy to treat cancers. Herein we present a series of long double-stranded multiplex small interfering RNAs (multi-siRNAs) that is suitable for dual genes silencing through a sequence-specific RNA interference process without inducing significant immune responses. A gap feature structurally designed in either of the nucleotide strands of the multi-siRNAs was proved to be essential toward silencing target genes and avoiding immune responses. Furthermore, the silencing effect of multi-siRNAs against *SURVIVIN* and *BCL-2* genes was shown to be effective and resulted in up-regulation of caspase-3 related apoptosis and, in turn, inhibition of bladder cancer cell proliferation. Our observation suggested that the rationally designed multi-siRNAs would have great potential for therapeutic siRNA design.

Introduction

RNA interference (RNAi) is a gene silencing mechanism induced by double-stranded RNA (dsRNA). Naturally, when long dsRNA is introduced into cells, Dicer, a cytoplasmic RNase 3 enzyme, cleaves it into 21- to 23-bp dsRNA with 2-nt 3′ overhangs, which is termed small interfering RNA (siRNA) (Zamore et al., 2000). RNA-induced silencing complex (RISC) loads the antisense strand of siRNA then recognizes and cleaves target messenger RNAs (mRNAs) with complementary sequences, which results in effective gene silencing (Elbashir et al., 2001).

Because of its efficient and specific silencing of target gene expression, siRNA has recently been experimentally used to treat cancers. In general, inhibition of a single oncogenic gene is insufficient to kill tumor cells because oncogenesis is associated with multiple genes involved in multiple pathways (Menendez et al., 2004). Therefore, use of multi-targeting siRNAs could be an advantageous strategy, by which expression of multiple genes can be inhibited simultaneously, and thus this may lead to more effective anticancer therapies than what single-targeting siRNA could achieve. In addition to multi-cassette short hairpin RNAs (shRNAs) (Watanabe et al., 2006) and long hairpin RNAs (Sano et al., 2008), studies on the use of synthetic multi-targeting siRNAs have also been reported. Hossbach et al. (Hossbach et al., 2006) reported a dual-targeting siRNA that was composed of 2 fully target-complementary guide strands with the strands partially complementary to each other. An algorithm was further developed to predict dual-targeting siRNAs with complete complementary strands that acted as active guide strands separately targeting different mRNAs (Tiemann et al., 2010). However, both methods suffered from limitation of the algorithm used, and the designed siRNAs may not be the most effective sequences. A recent study reported that long synthetic siRNA duplexes (38 bp) simultaneously knocked down expression of 2 genes without triggering an interferon response (Chang et al., 2009). This, however, contradicted the results from a previous study, in that dsRNAs longer than 30 bp could not execute specific gene silencing due to an induction of interferon response (Elbashir et al., 2001).

In the present study, we designed a group of new and long double-stranded multiplex siRNA (multi-siRNA) structures, featured with a gap in either sense strand or antisense strand. Results proved that the uniquely designed multi-siRNAs were capable of silencing both *SURVIVIN* and B-cell lymphoma 2 (*BCL-2*) genes effectively in an Argonaute-2 (*AGO2*)-dependent manner without interferon responses, thus significantly suppressed proliferation of human bladder cancer T24 cells.

Materials and Methods

Sequence design of single-targeting siRNAs and multiplex-siRNAs

Individual siRNAs targeting human *SURVIVIN* mRNA (si-S1 ~ si-S3) were selected from a full-site siRNA library of *SURVIVIN* constructed by Biomics Biotechnologies Co. Ltd. Individual siRNAs targeting human *BCL-2* (si-B1 and si-B2) were designed using Thermo siDESIGN Center and Invitrogen BLOCK-iT RNAi Designer online tools. After screening the most effective single-target siRNA sequences, multi-target

[1]Biomics Biotechnologies Co., Ltd., Nantong, Jiangsu, China.
[2]State Key Laboratory of Natural and Biomimetic Drugs, School of Pharmaceutical Sciences, Peking University, Beijing, China.

siRNAs were designed using the sequences listed in Table 1 accordingly. To enhance stability of the multi-target siRNAs, 2′-OMe modification was incorporated in both of the strands on every second nucleotide (Czauderna et al., 2003). siRNA targeting luciferase gene (si-GL3) was used as a negative control. All siRNAs in the study were chemically synthesized by Biomics Biotechnologies.

Cell culture and siRNA transfection

T24 cells were conserved in Biomics and maintained in RPMI-1640 medium supplemented with 10% fetal bovine serum, 100 units/mL penicillin, and 100 μg/mL streptomycin at 37°C under 5% CO_2 humidified atmosphere. Cells grown to a confluence of 30%–40% were transfected with siRNAs by Lipofectamine 2000 according to manufacturer's guidelines. Ten nanomoles of siRNA was used in each case unless stated otherwise.

Quantitative real-time reverse transcription polymerase chain reaction

A RISO™ RNA isolation reagent (Biomics Biotech) was used to extract total RNA from cell lysates. The complementary DNA was synthesized by reverse transcription and expression levels of human *SURVIVIN and BCL-2* mRNA were determined by quantitative real-time reverse transcription polymerase chain reaction (qRT-PCR) using EzOmics™ one-step qPCR kit (Biomics Biotech) according to manufacturer's instructions. Specific primers used for each gene were as follows:

SURVIVIN forward: 5′-AGGTCATCTCGGCTGTTCCTG-3′
SURVIVIN reverse: 5′-TCATCCTCACTGCGGCTGTC-3′
BCL-2 forward: 5′-GGCTGGGATGCCTTTGTG-3′
BCL-2 reverse: 5′-GCCAGGAGAAATCAAACAGAGG-3′
OAS1 forward: 5′-GTGAGCTCCTGGATTCTGCT-3′
OAS1 reverse: 5′-TGTTCCAATGTAACCATATTTCTGA-3′
IFIT1 forward: 5′-AAAAGCCCACATTTGAGGTG-3′

Table 1. Small Interfering RNA Sequences and Modifications

siRNA	*Sequence*
si-S3	5′ GACUUGGCCCAGUGUUUCU 3′ 3′ CUGAACCGGGUCACAAAGA 5′
si-B1	5′ GGAUGACUGAGUACCUGAA 3′ 3′ CCUACUGACUCAUGGACUU 5′
Sub-1	5′ GACUUGGCCCAGUGUUUCUACUGGAUGA CUGAGUACCUGAA 3′ 3′ CUGAACCGGGUCACAAAGA CCUACUGAC UCAUGGACUU 5′
Sub-2	5′ GACUUGGCCCAGUGUUUCU GGAUGACU GAGUACCUGAA 3′ 3′ CUGAACCGGGUCACAAAGAUGACCUACU GACUCAUGGACUU 5′
Sub-3	5′ GACUUGGCCCAGUGUUUCUACUGGAUGA CUGAGUACCUGAA 3′ 3′ CUGAACCGGGUCACAAAGAUGACCUACU GACUCAUGGACUU 5′
si-GL3	5′ CUUACGCUGAGUACUUCGAdTdT 3′ 3′ dTdTGAAUGCGACUCAUGAAGCU 5′

2′-O-methyl ribonucleotide modifications are underlined.
siRNA, small interfering RNA.

IFIT1 reverse: 5′-GAAATTCCTGAAACCGACCA-3′
AGO2 forward: 5′-CGACTGCTAGGTCGGCGCC-3′
AGO2 reverse: 5′-TCCCAGACGCCCTGGACAGG-3′
GAPDH forward: 5′-GAAGGTGAAGGTCGGAGTC-3′
GAPDH reverse: 5′-GAAGATGGTGATGGGATTTC-3′

Samples were tested in triplicate and glyceraldehyde 3-phosphate dehydrogenase (*GAPDH*) expression was used as an internal control.

Western blotting

Cells were seeded in 6-well plates respectively. When confluence of the cells reached 50%, transfection was conducted with siRNA and lipofectamine 2000 as described above. After further incubation for 48 hours, the cells were lysed using a mammalian cell total protein lysis buffer (Sangon Biotech). Fifty micrograms of total proteins were separated in 12% sodium dodecyl sulfate acrylamide gels and electroblotted onto an immobilon polyvinylidene difluoride membrane (Millipore, Billerica). The membranes were blocked for 2 hours in phosphate buffered saline with Tween-20 (PBST) containing 5% skim milk powder and incubated overnight at 4°C with a 1:100 dilution of mouse monoclonal primary antibody to human SURVIVIN (Santa Cruz Biotech) or a 1/200 dilution of mouse monoclonal antibody to human BCL-2 (Santa Cruz Biotech) and human GAPDH (Santa Cruz Biotech), respectively. The membranes were then washed in PBST and incubated with a 1/1000 dilution of goat anti-mouse horseradish peroxidase–conjugated secondary antibody (Jackson ImmunoResearch) at room temperature for 2 hours. Upon incubation with an electrochemiluminescence (ECL) chemiluminescence reagent (Beyotime Institute of Biotechnology), the membranes were exposed to films (Kodak).

Interferon responses assay

Transfection and qRT-PCR assays were performed as described above. Expression of 2′-5′-oligoadenylate synthetase 1 *(OAS1)* and interferon-induced protein with tetratricopeptide repeats 1 *(IFIT1)* mRNAs were measured. Expression of GAPDH was used as an internal control for normalization of qRT-PCR results.

Cell proliferation assay

Cells were seeded in 96-well plates at 2,000 cells per well 24 hours prior to transfection, and the transfection was conducted as described above. At the scheduled time points, cell proliferation capacity was measured in triplicate using a cell counting kit according to manufacturer's specifications (Beyotime Institute of Biotechnology).

Apoptosis analysis

To measure early and late apoptotic cells, the cell samples were stained with fluorescein isothiocyanate (FITC)-conjugated Annexin V and propidium iodide using an Annexin V-FITC Apoptosis Detection kit (KeyGen Biotech) and analyzed by FACScan flow cytometry (BD Biosciences) at 48 hours after siRNA transfection.

Caspase-3 activity assay

Total proteins were extracted from transfected cells using a mammalian cell total protein lysis buffer (Sangon Biotech) as

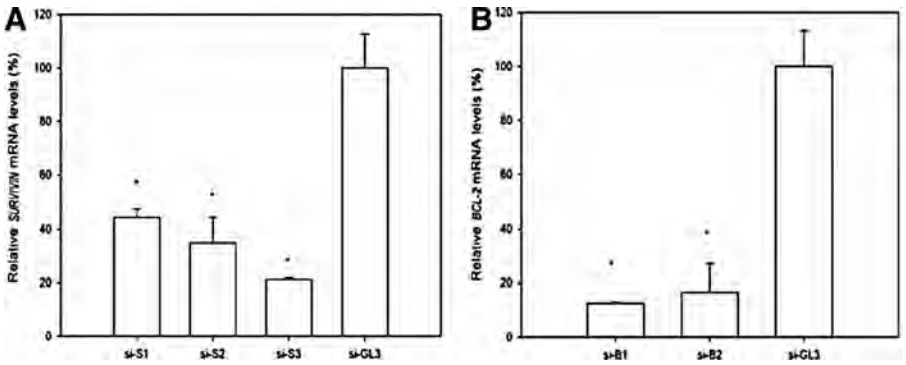

FIG. 1. Selection of effective small interfering (siRNAs) against *SURVIVIN* and B-cell lymphoma 2 (*BCL-2*) genes. siRNAs targeting human *SURVIVIN* gene are named si-S1, si-S2, and si-S3. si-B1 and si-B2 represent siRNAs targeting human *BCL-2* gene. si-GL3 is a siRNA silencing luciferase gene and served as a negative control. Quantitative real-time polymerase chain reaction (q-RT-PCR) was performed for siRNAs against either *SURVIVIN* mRNA **(A)** or *BCL-2* mRNA **(B)** 48 hours after transfection. Values were averaged from 3 independent experiments. * indicates significant difference compared with values for si-GL3 treated cells ($P < 0.05$).

described above. Protein concentration of the whole cell extract was measured by Bradford assay. Activity of caspase-3 was determined using a caspase-3 activity kit (Beyotime Institute of Biotechnology) according to manufacturer's instructions. One unit of caspase-3 activity is defined as the amount of enzyme that cleaves 1.0 nmol of colorimetric substrate Ac-DEVD-pNA at a saturated substrate concentration at 37° in 1 hour. Relative caspase-3 activities were expressed as folds of up-regulation compared to those of si-GL3 transfected cells.

Statistical analysis

Data were expressed as means ± standard deviation. Difference between any 2 groups was determined by one-way analysis of variance and is considered to be significant statistically when P value is < 0.05.

Results

Selection of effective siRNA targeting human SURVIVIN or BCL-2

Designed siRNAs targeting human *SURVIVIN* gene (si-S1 ~ si-S3) and human *BCL-2* gene (si-B1 and si-B2) were first screened for their effectiveness, respectively. As shown in Fig. 1, si-S3 transfection resulted in a significant decrease in expression of *SURVIVIN* mRNA, at 79%, compared with that in the negative control, and si-B1 was found to be the most effective siRNA targeting *BCL-2* gene with 84% gene knockdown. The results were further confirmed by western blotting analysis (Fig. 2), in which si-S3 and si-B1 significantly suppressed the expression of SURVIVIN and BCL-2 proteins respectively.

Effects of multi-siRNAs on BCL-2 and SURVIVIN gene expression

Three unique types of double stranded multi-siRNA structures were designed and synthesized, as shown in Table 1, using the sequences of si-S3 and si-B1 in combination, which were named Sub-1, Sub-2, and Sub-3, respectively. To evaluate their gene silencing efficiency, Sub-1, Sub-2, and Sub-3 were transfected, respectively, into T24 cells by lipofectamine 2000. Expression levels of mRNA and protein from *SURVIVIN* and *BCL-2* genes were determined by qRT-PCR and western blotting assays, respectively. For the cells treated with Sub-1, simultaneous down-regulations of *SURVIVIN* mRNA to about 66% and *BCL-2* mRNA to 83% were achieved, respectively. In comparison, Sub-2 showed somewhat similar down-regulations of *SURVIVIN* (71%) and *BCL-2* (81%) at mRNA levels (Fig. 3). Western blotting assays further demonstrated that both Sub-1 and Sub-2 inhibited the expression of *SURVIVIN* and *BCL-2* proteins more effectively than Sub-3 (Fig. 4). In light of these results, further studies were focused on the use of the more effective multi-siRNAs, Sub-1, and Sub-2.

No significant interferon responses induced by multi-siRNAs

It was previously known that dsRNA longer than 30 bp (Elbashir et al., 2001) could induce interferon (IFN) responses

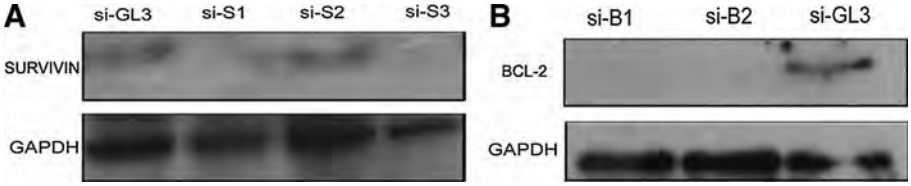

FIG. 2. Suppression in protein levels of *SURVIVIN* or *BCL-2* gene by siRNAs in T24 cells. **(A)** Suppression of SURVIVIN by SURVIVIN-specific siRNAs treatment. **(B)** Suppression of BCL-2 by BCL-2-specific siRNAs treatment. si-S1, si-S2, si-S3, si-B1, si-B2, and si-GL3 siRNAs are defined as in Fig. 1.

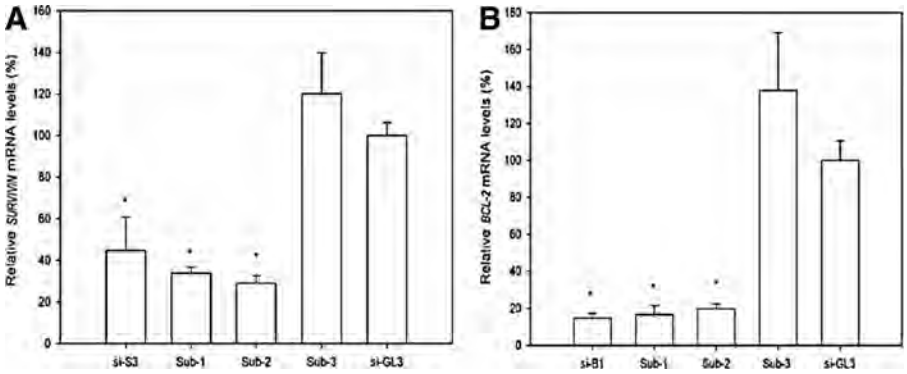

FIG. 3. Gene-silencing activities of multi-siRNAs against *SURVIVIN* and *BCL-2* genes. siRNAs were transfected into T24 cells by lipofectamine 2000. Twenty-four hours after transfection, *SURVIVIN* **(A)** or *BCL-2* **(B)** mRNA levels were quantified by q-RT-PCR. Sub-1 and Sub-2: long double-stranded multi-siRNAs targeting *SURVIVIN and BCL-2* genes with a gap in the antisense strand or the sense strand, respectively. Sub-3: the long double-stranded siRNA targeting *SURVIVIN* and *BCL-2* genes with intact sense and antisense strands. si-S3 (targeting *SURVIVIN*) and si-B1(targeting *BCL-2*) served as individual siRNA controls. si-GL3 is a siRNA silencing luciferase gene and served as a negative control. All data represent means ± standard deviation (SD) of 3 independent experiments. * indicates significant difference in levels compared with si-GL3 treated cells ($P < 0.05$).

and thus cause non-specific apopotosis (fasle gene knock-down). To assess if a potential influence of IFN response happened on the multi-siRNAs (Sub-1 and Sub-2) mediated gene silencing effects, the RNA-transfected cells were analyzed for mRNA expressions of *OAS1* and *IFIT1* at 48 hours after the transfection, along with the si-S3 and si-B1 (siRNAs < 21bp) treated cells as negative controls. As shown in Fig. 5, similar to si-S3 or si-B1 negative controls, the mRNA expressions of *OAS1* and *IFIT1* were not significantly increased in the Sub-1 and Sub-2 transfected cells. In contrast, significant increases in *OAS1* and *IFIT1* mRNA expressions were only observed in the Sub-3 transfected cells, reaching 1.8-fold and 5.4-fold higher than negative control, respectively.

Gene silencing by multi-siRNAs in an AGO2-dependent manner

To study whether the multi-siRNAs silence the genes via the same *AGO2*-dependent pathway as that of conventional siRNAs, knock-down of *AGO2* expression was first implemented by a known effective siRNA (Fig. 6), and then mRNA levels of *SURVIVIN* and *BCL-2* genes were measured, respectively, after further transfection with targeting siRNAs or multi-siRNAs. As shown in Fig. 7, the knock-down of both *SURVIVIN* and *BCL-2* genes by either individual siRNAs (si-S3 and si-B1) or multi-siRNAs (Sub-1 and Sub-2) was effectively blocked after pretreatment of cells with *AGO2* gene-specific siRNA. The result supported that the effect of gene silencing achieved by the multi-siRNAs did follow an *AGO2*-dependent pathway.

Inhibition of cell proliferation by multi-siRNAs

At 48, 72, 96, and 120 hours after transfection, inhibition of cell proliferation was observed in all the targeting siRNA groups compared to the negative control group (Fig. 8). At 48 hours after the treatment with 10 or 20 nM of si-S3, the relative proliferation rates of T24 cells were 80.36% ± 5.61% and 57.82% ± 11.85%, respectively ($P < 0.05$, compared to the si-GL3 control). The same trend was also observed in si-B1, Sub-1, and Sub-2 transfected groups, in which the relative proliferation rates decreased with an increased amount of the siRNAs used. The results indicated that the effect on growth inhibition was siRNA dose-dependent. Furthermore, it was noted that the inhibitory effect of the siRNAs was also time-dependent to a certain extent. For instance, cells transfected with Sub-1 for 48, 72, 96, and 120 hours showed a relative viability in rates, distributed at 31.21% ± 2.29%, 23.24% ± 2.36%, 27.30% ± 0.96%, and 14.55% ± 0.40%, respectively. In addition, it was also observed that at the higher dose of 20 nM, the multi-siRNAs (Sub-1 and Sub-2) transfection produced greater suppression activity than either single-target siRNAs (si-S3 and si-B1) or the combination of si-S3 and si-B1 (10 nM + 10nM) treatment ($P < 0.05$) at all the measuring time points.

Enhancement of cell apoptosis by multi-siRNAs

Since *SURVIVIN* and *BCL-2* are known as the anti-apoptosis genes, blocking of *SURVIVIN* or *BCL-2* gene is expected to cause an increase in apoptosis (Kunze et al., 2008; Montazeri et al, 2011). Rates of apoptosis were measured in T24 cells after treatment with siRNAs by flow cytometry assays.

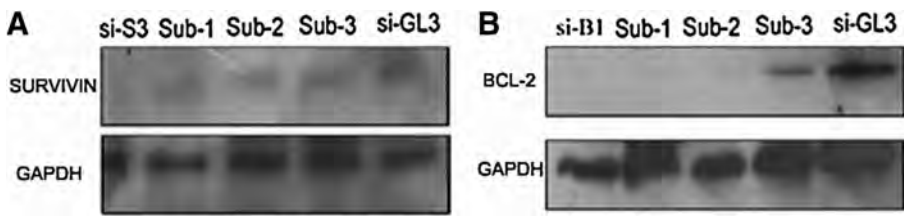

FIG. 4. Suppression of *SURVIVIN* **(A)** and *BCL-2* **(B)** expression by multi-siRNAs. si-S3, si-B1, Sub-1, Sub-2, Sub-3, and si-GL3 siRNAs are defined as in Fig. 3.

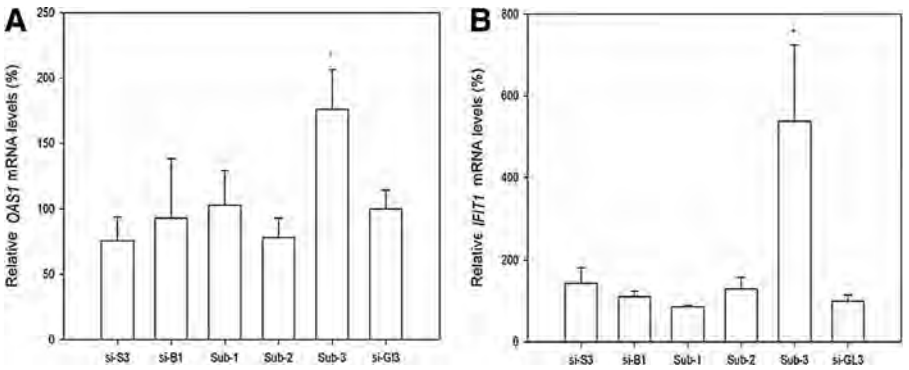

FIG. 5. Interferon responses triggered by siRNAs. **(A)** Oligoadenylate synthetase 1 (*OAS1*) mRNA levels in T24 cells induced by siRNA transfection. **(B)** Tetratricopeptide repeats 1 (*IFIT1*) mRNA levels in T24 cells transfected with siRNAs. si-S3, si-B1 si-GL3, Sub-1, Sub-2, and Sub-3 siRNAs are defined as in Fig. 3. Data were averaged from 3 independent experiments. $^*P < 0.05$ compared with si-GL3 cells.

As shown in Fig. 9, individual si-S3 or si-B1 treatment produced an augmentation of apoptosis to 20.96% and 18.45%, respectively, compared with the negative control, which displayed an apoptosis rate of 6.35%. An increase in apoptosis rate induced by the multi-siRNAs was also observed. The apoptosis in Sub-1 and Sub-2 treatments reached to 18.63% and 23.63%, respectively.

Up-regulation of caspase-3 activity by multi-siRNAs

It is known that apoptosis involves a cascade of proteolytic reactions affected mainly by the caspase family, and caspase-3 is thought to be the major executor of apoptosis (Porter and Janicke, 1999). Therefore, the levels of the caspase-3 activity were analyzed after siRNA treatments, as shown in Fig. 10. Based on apoptotic caspase-3 activity, the si-S3 and si-B1 transfection groups reached 1.57-fold and 1.77-fold increases in apoptosis respectively, compared with the si-GL3 transfection group ($P < 0.05$); whereas, Sub-1 and Sub-2 treatment groups demonstrated much greater increases in caspase-3 activities (3.70-fold and 3.64-fold higher than si-GL3 control, respectively, $P < 0.05$).

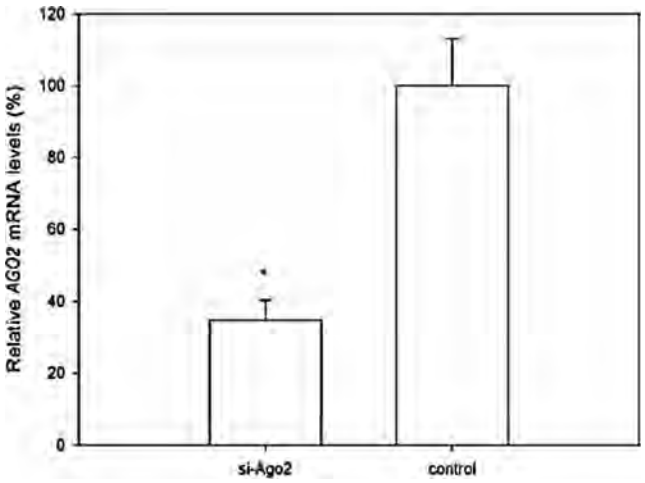

FIG. 6. Gene-silencing activity of si-Argonaute-2 (*AGO2*) against *AGO2* gene. *AGO2* mRNA level was quantified by q-RT-PCR after si-Ago2 transfection. All data represent means ± SD of 3 independent experiments. $^*P < 0.05$ compared with si-GL3 treated cells.

Discussion

In the present study, we designed 2 new multi-siRNA structures composed of an intact long strand (at least 30 nucleotides in length) and 2 complementary shorter strands. There is a gap between the 2 shorter strands, which results in the segmentation of the complementary strand. A variety of multi-siRNAs targeting human *SURVIVIN* and human *BCL-2* genes was synthesized, and the results proved that Sub-1 and Sub-2 with a gap in either of the strands could effectively silence 2 target genes simultaneously with high potency compared with the corresponding single-target siRNAs. In contrast, gene knock-down efficacy of long double-stranded siRNA (Sub-3) was poor (Figs. 3, 4), although there was no difference in the nucleotide sequences between Sub-3 and Sub-1 (or Sub-2). The results indicated that the gap in either antisense or sense strand is essential to the silencing activities of the multi-siRNAs, and knock-down potency of the multi-siRNAs depends on the specific structures to a certain extent. It is well known that long dsRNA in cells will serve as substrates to be digested by a dsRNA-specific endonuclease, Dicer, into siRNA duplexes as functional effectors to cleave target mRNAs. Therefore, the gap between the two complementary strands may provide recognizable sites and/or facilitate the process of Dicer, thus the resultant two siRNAs would then silence their targets, respectively. However, an exact mechanism remains unclear and requires further studies.

A preliminary study on the mechanism of specific gene silencing effects induced by the multi-siRNAs was further studied. It has been widely accepted that siRNA-directed RNA interference is mediated by *AGO2*. As a core component of RISC, AGO2 protein functions as a slicer to cleave target mRNA and offers a binding site for siRNA in RISC assembly (Liu et al., 2004; Rand et al., 2005). Therefore, the function of AGO2 on the multi-siRNAs induced gene silencing was investigated. As shown in Fig. 7, the gene silencing effects of the multi-siRNAs were blocked when expression of the *AGO2* gene was down regulated. Thus it can be concluded that the silencing effect induced by the multi-siRNAs also requires AGO2 as a catalysis and is likely to be *AGO2*-dependent, and it follows the same pathway as that utilized by conventional siRNAs.

A previous study reported that dsRNA longer than 30 bp could not execute specific gene silencing because of induction of significant interferon responses after being transfected into mammalian cells (Elbashir et al., 2001). IFIT1 was identified as a gene that was most strongly induced in response to

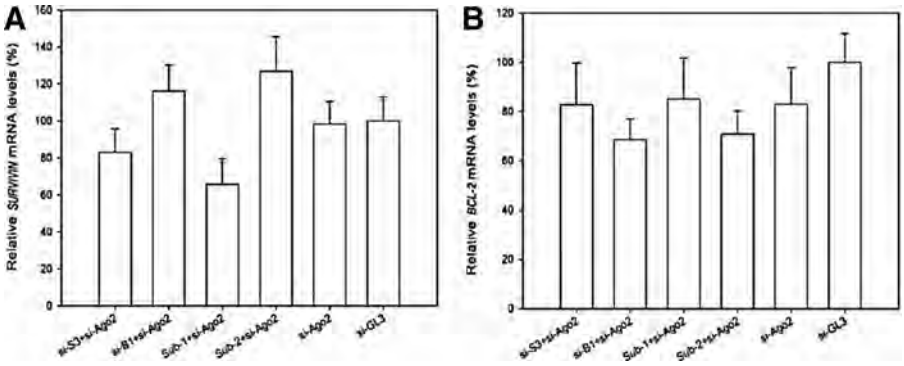

FIG. 7. Multi-siRNAs trigger gene silencing in an *AGO2*-dependent manner. Relative *SURVIVIN* **(A)** and *BCL-2* **(B)** mRNA levels were determined by q-RT-PCR after indicated siRNAs treatment following *AGO2* mRNA knock-down (si-Ago2 transfection). si-S3, si-B1, si-GL3, Sub-1, and Sub-2 siRNAs are defined as in Fig. 3. Values represent the means averaged from 3 independent experiments.

treatment with dsRNA (Geiss et al., 2001). In addition, *OAS1*, a classical interferon target gene, could be induced by both type 1 and type 2 IFNs (Eskildsen et al., 2003). Therefore, *OAS1* and *IFIT1* were used in this study as sensitive biomarkers to evaluate immune responses resulted from dsRNA. The levels of *OAS1* and *IFIT1* mRNAs from the multi-siRNAs treated T24 cells were measured against those from a conventional siRNA, which was used as a control. The results indicated that the multi-siRNAs with a gap in either of the strands did not evoke significant interferon responses, nor did single-target siRNAs. However, long double-stranded RNA (Sub-3) transfection induced significant increase in the *IFIT1* and *OAS1* mRNA levels, although Sub-3 is also selectively modified by 2'OMe nucleotides. Therefore, a conclusion could be drawn that the lack of an immune response from the multi-siRNAs was due to the specific structures to some extent. These findings demonstrated that *in vitro* gene silencing activities of the multi-siRNAs against respective target genes were derived from sequence-specific RNA interference rather than an IFN response.

A presently accepted notion is that anticancer agents are effective to lead to death of tumor cells only when they induce apoptosis. However, apoptosis is frequently dysregulated in tumor cells, by which cancer cells become resistant to anticancer drug treatments. Overexpression of anti-apoptotic genes, such as *BCL-2* and *SURVIVIN*, has been shown to play a critical role in deficiency of apoptosis (Kasibhatla and Tseng, 2003; Varfolomeev and Vucic, 2011). In the study, multi-siRNAs (Sub-1 and Sub-2) targeting *SURVIVIN* and *BCL-2* genes simultaneously was designed in an attempt to mitigate the apoptosis deficiency on bladder cancer T24 cells. The data revealed that suppression of either *SURVIVIN* or *BCL-2* gene individually resulted in a small decrease in cell growth and a modest increase in spontaneous cell apoptosis. In contrast, when simultaneous suppression of both *SURVIVIN* and *BCL-2* genes was achieved by Sub-1 or Sub-2, the proliferation of T24 cells was dramatically inhibited and the apoptosis was enhanced by a significant activation of caspase-3. Therefore, the effects of Sub-1 and Sub-2 against cancer cell growth could be related to apoptosis induction.

It can also be noted that the multi-siRNAs with a gap in either of the strands were demonstrated to be more effective on inhibition of cancer cell growth than individual siRNAs used either alone or as a cocktail in the present experiment. There might be two reasons that could account for the improvement: (1) It was previously reported that co-transfection of siRNAs could result in reduced knock-down activity because of competition between siRNAs (Tanudji et al., 2010); therefore, the activity of some siRNAs within the cocktail may be reduced, which could attenuate the effects of the mixture. (2) The multi-siRNAs were transfected into cells as an intact molecule and were then cleaved by Dicer into 2 separate siRNAs to silence respective targets in the same cell. A recent comparison of the efficacy of Dicer intact substrate RNAs and chemically synthesized non-Dicer substrate siRNAs shows that both triggers are potent in target-gene silencing. Differences could, however, be seen when comparing specificity. Many non-Dicer substrate siRNA molecules are easily to produce an off-target effect, whereas the mixture of Dicer intact substrate RNAs leads to a more specific knockdown

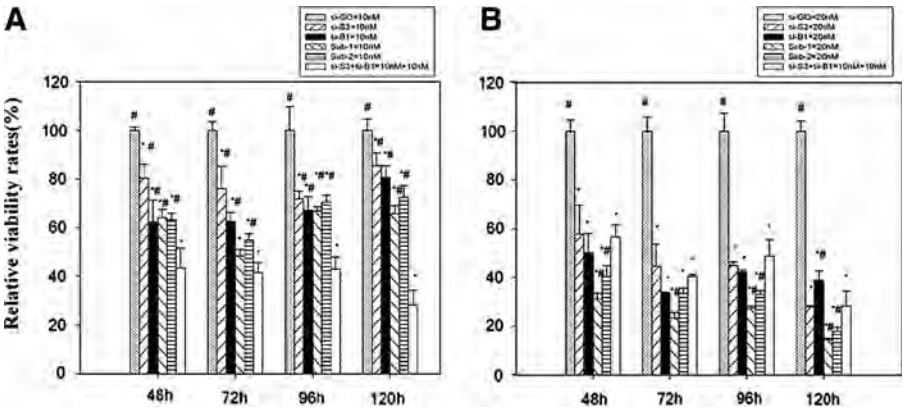

FIG. 8. Relative viability of T24 cells after siRNA treatments. T24 cell proliferation was analyzed by a cell counting kit 8 assay at the indicated time points after **(A)** 10 nM or **(B)** 20nM siRNA transfection. si-S3, si-B1, si-GL3, Sub-1, and Sub-2 siRNAs are defined as in Fig. 3. Cell proliferation following siRNA treatment was normalized to that of si-GL3 treatment. $^{*}P < 0.05$ compared with the negative control siRNA (si-GL3) group. $^{\#}P < 0.05$ compared with the mix of si-S3 (10 nM) and si-B1 (10 nM) combination group.

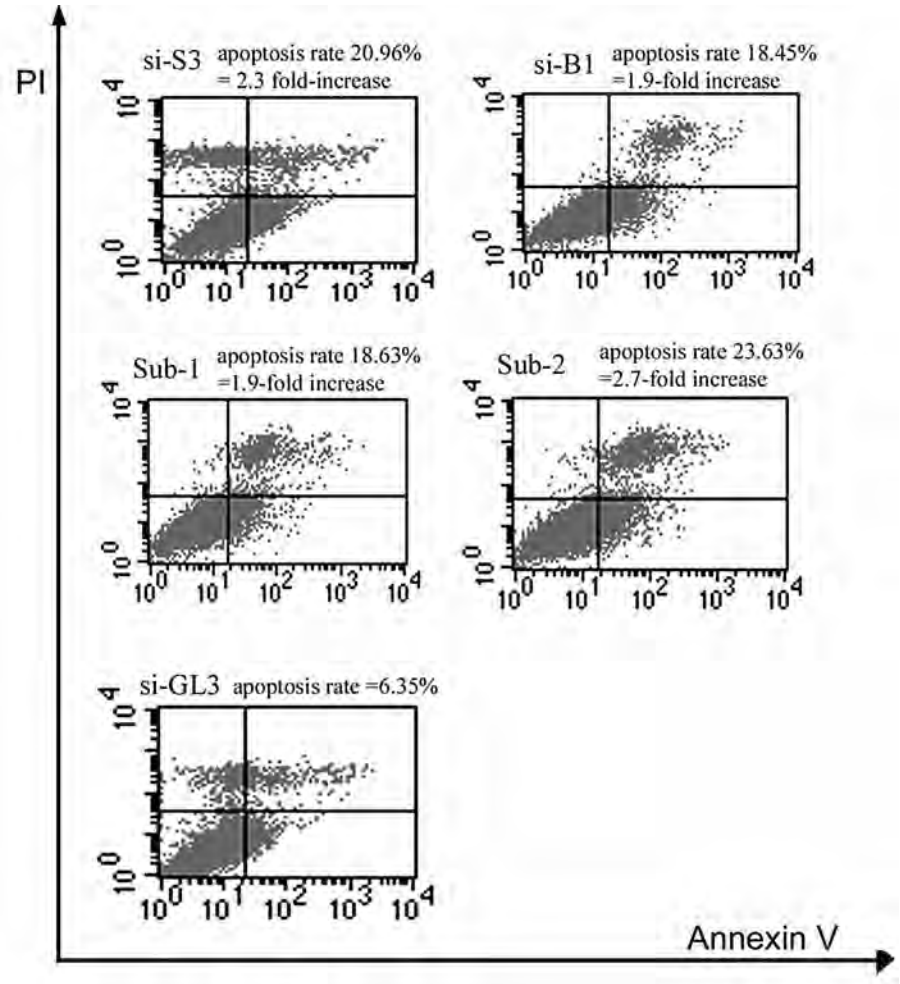

FIG. 9. Induction of apoptosis in T24 cells 48 hours after siRNA treatment. Apoptosis rates were measured by fluorescence activated cell sorting analysis after AnnexinV-propidium iodide (PI) staining. Percentage of apoptotic cells included both early- and late-stage apoptosis (AV+/PI− and AV+/PI+). Increases in apoptosis were calculated relative to si-GL3 control. si-S3, si-B1, si-GL3, Sub-1, and Sub-2 siRNAs are defined as in Fig. 3.

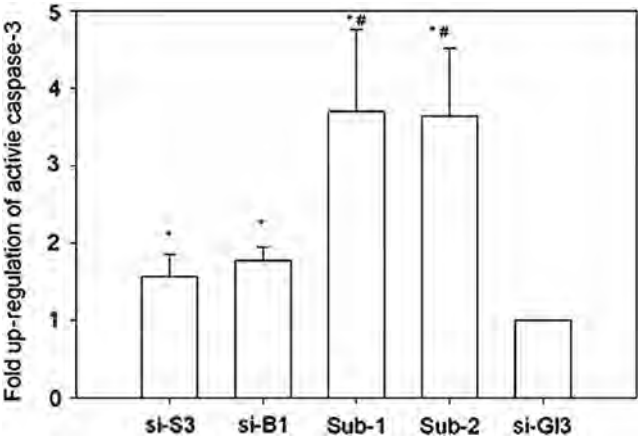

FIG. 10. Activity of caspase-3 increased after siRNA transfection. Activity of caspase-3 was quantified by colorimetric assay and normalized to that of the si-GL3 control group. Values were averaged from three independent experiments. $^{*}P < 0.05$ compared with si-GL3 group; $^{\#}P < 0.05$ compared with si-S3 group. si-S3, si-B1, si-GL3, Sub-1, and Sub-2 siRNAs are defined as in Fig. 3.

(Kittler et al., 2007). The efficiency of gene silencing primarily relies on the optimal incorporation of siRNA into RISC, where the Dicer substrate RNAs have a preference for RISC loading as a consequence of the physical transfer of the processed siRNA from Dicer (Amarzguioui et al., 2008). Therefore, it was probably on these reasons that multi-siRNAs used in the present experiment showed more effective activity than individual siRNA mixture.

In summary, it was demonstrated that the multi-siRNAs could be potentially utilized for attaining silencing of multiple genes without eliciting an immune response, and the unique design of a gap in either sense strand or anti-sense strand in the multi-siRNAs was proved to be necessary to knock down multiple genes and to avoid immune responses. The results also revealed that the gene knock-down effects resulted from the multi-siRNAs were derived from sequence-specific RNA interference rather than an IFN response. Furthermore, the designed multi-siRNAs targeting both *SURVIVIN* and *BCL-2* genes dramatically inhibited cell growth on bladder cancer T24. Therefore, this new type of multi-siRNAs may have a great potential toward siRNA-based therapeutic applications.

Acknowledgments

The project was supported by Postdoctoral Sustentation Foundation of Jiangsu Province, China (grant no: 1001052C)

and Medicine Program of Nantong Science and Technology Bureau, China (grant no. AS2010010).

Author Disclosure Statement

No competing financial interests exist.

References

AMARZGUIOUI, M., and ROSSI, J.J. (2008). Principles of Dicer substrate (D-siRNA) design and function. Methods Mol. Biol. **442,** 3–10.

CHANG, C.I., KANG, H.S., BAN, C., KIM, S., and LEE, D.K. (2009). Dual-target gene silencing by using long, synthetic siRNA duplexes without triggering antiviral responses. Mol. Cell. **27,** 689–695.

CZAUDERNA, F., FECHTNER, M., DAMES, S., AYQUN, H., KLIPPEL, A., PRONK, G.J., GIESE, K., and KAUFMANN, J. (2003). Structural variations and stabilizing modifications of synthetic siRNAs in mammalian cells. Nucleic Acids Res. **31,** 2705–2716.

ELBASHIR, S.M., HARBORTH, J., LENDECKEL, W., YALCIN, A., WEBER, K., and TUSCHL, T. (2001). Duplexes of 21-nucleotide RNAs mediate RNA interference in cultured mammalian cells. Nature **411,** 494–498.

ESKILDSEN, S., JUSTESEN, J., SCHIERUP, M.H., and HARTMANN, R. (2003). Characterization of the 2′-5′-oligoadenylate synthetase ubiquitin-like family. Nucleic Acids Res. **31,** 3166–3173.

GEISS, G., JIN, G., GUO, J., BUMGARNER, R., KATZE, M.G., and SEN, G.C. (2001). A comprehensive view of regulation of gene expression by dsRNA mediated cell signaling. J. Biol. Chem. **276,** 30178–30182.

HOSSBACH, M., GRUBER, J., OSBORN, M., WEBER, K., and TUSHL, T. (2006). Gene silencing with siRNA duplexes composed of target-mRNA-complementary and partially palindromic or partially complementary single-stranded siRNAs. RNA Biol. **3,** 82–89.

KASIBHATLA, S., and TSENG, B. (2003). Why target apoptosis in cancer treatment? Mol. Cancer Ther. **2,** 573–580.

KITTLER, R., SURENDRANATH, V., HENINGER, A.K., SLABICHI, M., THEIS, M., PUTZ, G., FRANKE, K., CALDARELLI, A., GRABNER, H., KOZAK, K., et al. (2007). Genome-wide resources of endoribonuclease-prepared short interfering RNAs for specific loss-of-function studies. Nat. Methods **4,** 337–344.

KUNZE, D., WUTTIG, D., FUESSEL, S., KRAEMER, K., KOTZSH, M., MEYE, A., GRIMM, M.O., HAKENBERG, O.W., and WIRTH, M.P. (2008). Multitarget siRNA inhibition of antiapoptotic genes (XIAP, BCL2, BCL-X(L)) in bladder cancer cells. Anticancer Res. **28,** 2259–2263.

LIU, J., CARMELL, M.A., RIVAS, F.V., MARSDEN, C.G., THOMSON, J.M., SONG, J.J., HAMMOND, S.M., JOSHUA-TOR, L., and HANNON, G.J. (2004). Argonaute 2 is the catalytic engine of mammalian RNAi. Science **305,** 1437–1441.

MENENDEZ, J.A., VELLON, L., MEHMI, I., OZA, B.P., ROPERO, S., CLOLMER, R., and LUPU, R. (2004). Inhibition of fatty acid synthase (FAS) suppresses HER2/neu (erbB-2) oncogene overexpression in cancer cells. Proc. Natl. Acad. Sci. U. S. A. **101,** 10715–10720.

MONTAZERI ALIABADI, H., LANDRY, B., MAHDIPOOR, P., and ULUDAG, H. (2011). Induction of apoptosis by survivin silencing through siRNA delivery in a human breast cancer cell line. Mol. Pharm. **8,** 1821–1830.

PORTER, A.G., and JANICKE, R.U. (1999). Emerging roles of caspase-3 in apoptosis. Cell. Death Differ. **6,** 99–104.

RAND, T.A., PETERSEN, S., DU, F., and WANG, X. (2005). Argonaute 2 cleaves the anti-guide strand of siRNA during RISC activation. *Cell* **123,** 621–629.

SANO, M., LI, H., NAKANISHI, M., and ROSSI, J.J. (2008). Expression of long anti-HIV-1 hairpin RNAs for the generation of multiple siRNAs: advantages and limitations. Mol. Ther. **16,** 170–177.

TANUDJI, M., MACHALEK, D., ARNDT, G.M., and RIVORY, L. (2010). Competition between siRNA duplexes: impact of RNA-induced silencing complex loading efficiency and comparison between conventional-21bp and Dicer-substrate siRNAs. Oligonucleotides **20,** 27–32.

TIEMANN, K., HOHN, B., EHSANI, A., FORMAN, S.J., ROSSI, J.J, and SAETROM, P. (2010). Dual-targeting siRNAs. RNA **16,** 1275–1284.

VARFOLOMEEV, E., and VUCIC, D. (2011). Inhibitor of apoptosis proteins: fascinating biology leads to attractive tumor therapeutic targets. Future Oncol. **7,** 633–648.

WATANABE, T., SUDOH, M., MIYAGISHI, M., AKASHI, H., ATAI, M., INOUE, K., TAIRA, K., YOSHIBA, M., and KOHARA, M. (2006). Intracellular-diced dsRNA has enhanced efficacy for silencing HCV RNA and overcomes variation in the viral genotype. Gene Ther. **13,** 883–892.

ZAMORE, P.D., TUSCHL, T., SHARP, P.A., and BARTEL, D.P. (2000). RNAi: double-stranded RNA directs the ATP-dependent cleavage of mRNA at 21 to 23 nucleotide intervals. Cell **101,** 25–33.

Address correspondence to:
York Yuanyuan Zhu, PhD
Biomics Biotechnologies Co., Ltd.
76 Changxing Road
E&T Development Area
Nantong 226016
China

E-mail: yzhu@biomics.cn

Received for publication January 5, 2013; accepted after revision April 8, 2013.

NUCLEIC ACID THERAPEUTICS
Volume 25, Number 1, 2015

DOI: 10.1089/nat.2014.0514

Size Unbiased Representative Enzymatically Generated RNAi (SURER) Library and Application for RNAi Therapeutic Screens

Tiejun Li,[1–3,*] York Yuanyuan Zhu,[1–3,*] Li Chen,[3,*] Yuncheng Sun,[1,2] Jian Yuan,[1,2] Michael Graham,[4] and Peter French[4]

RNA interference (RNAi) libraries screens have become widely used for small RNA (sRNA) therapeutic targets development. However, conventional enzymatically libraries, typically prepared using the type 2 restriction enzyme *Mme*I, produce sRNAs between 18 and 20 bp, much shorter than the usual lengths of 19–23 bp. Here we develop a size unbiased representative enzymatically generated RNAi (SURER) library, which employs type 3 restriction modification enzyme *EcoP15*I to produce sRNAs ranging from 19 to 23 bp using a group of rationally designed linkers, which can completely mimic the length of sRNAs naturally generated by Dicer enzyme in living cells, and the screening results of SURER libraries showed high recombination rate and knockdown efficiency. SURER library provides a useful tool for RNAi therapeutics screening in a fast and simple way.

Introduction

In recent years, screening of random libraries targeting particular genes has become an attractive and useful method to define small RNA (sRNA) therapeutics, including small interfering RNA (siRNA), short hairpin RNA (shRNA) [1–3], and other modified siRNAs [4]. Small RNA library-based approaches have several advantages for unknown sequence discovery, including immediate clone availability, cost-effectiveness over chemically synthesized RNA, and the potential to define siRNAs and/or shRNA constructs for long-term gene silencing based on sequences determined from such libraries [5–7].

Small interfering RNAs are a class of 19- to 23-bp double-stranded RNAs (dsRNAs) endogenously generated or artificially designed that trigger gene silencing via RNA interference (RNAi) pathways. RNAi can be induced by exogenously introduced [1] or endogenous siRNAs [8–10], the latter potentially derived from endogenous dsRNA precursors arising from ''natural'' processes such as bidirectional transcription, transcription of inverted repeats, or hybridization of pseudogene transcripts to mRNAs [11–14]. Once dsRNAs are processed by Dicer, siRNA duplexes enter the RNA-induced silencing complex, where conserved components including Argonaute (Ago) proteins unwind and cleave the passenger strand in the siRNA duplex, leaving the guide strand to pair with the target mRNA via perfect sequence complementarity, which in turn guides RNA cleavage [15].

MicroRNAs (miRNAs) are another class of endogenous sRNA (19–23 nt), which have been studied as regulators of gene expression in crucial biological processes, including cell development, differentiation, apoptosis, and proliferation [16,17]. MicroRNAs are post-transcriptional regulators that are processed from endogenously expressed transcripts [18,19] and have diverse functions in biology and disease.

RNA activation is a newly discovered mechanism of gene regulation triggered by small activating RNAs (saRNAs) that targets gene promoter regions instead of coding sequences and have been shown to activate the expression of endogenous genes [20–23], presenting a novel and natural tool for overexpressing functionally important genes for disease treatment.

Several strategies to enzymatically prepare shRNA libraries have been described, including EPRIL (enzymatic production of RNAi library) [24], REGS (restriction enzyme-generated siRNA) [25], SPEED (siRNA production by enzymatic engineering of DNA) [26], and others [27–30]. These are similar in principle but differ in details of their production. Typically, double-stranded (ds) complementary DNA (cDNA) is randomly cleaved into small fragments by

[1]Small RNA Technology and Application Institute and [3]Department of Pathological Anatomy, Nantong University, Nantong, China.
[2]Biomics Biotechnologies Co., Ltd., Nantong, China.
[4]Benitec Biopharma Ltd., Sydney, Australia.
*These authors contributed equally to this work.

*DNase*I (or restriction enzymes in some instances) and subsequently ligated to an artificial adaptor that contains an *Mme*I restriction site, which specifies cleavage 18–20 bp from the recognition site [31]. The generated siRNAs only have a maximum size of 20 bp [32]. However, siRNAs generated by Dicer in mammalian cells typically range from 21 to 23 bp; such sequences are therefore underrepresented in conventional libraries. Moreover, conventional approaches use polymerase chain reaction (PCR) amplification of palindromic structures, which can lead to reduction in library complexity and potential loss of the best therapeutic molecules [28]. Size unbiased representative enzymatically generated RNAi (SURER) libraries avoid these issues.

Materials and Methods

Construction of SURER Library

Complementary DNA fragments corresponding to coding sequences (CDSs) of hepatitis B virus (HBV) DNA polymerase, baculoviral IAP repeat-containing 5 (BIRC5), and a conserved domain the microphthalmia-associated transcription factor (MITF) conserved domain, were prepared by Biomics Biotechnologies Co., Ltd. Sequences of linkers and primers used for preparing SURER libraries are listed in Table 1, libraries were prepared using the procedures that follow.

Step 1. *DNase*I partial digestion. One hundred nanograms of the target cDNAs were partially digested to prepare 100–300 bp blunt-end fragments using 0.01–0.03 U *DNase*I (Roche) in a Mn^{2+} buffer at a final concentration of 10 mM Tris-HCl (pH 9.0), 2 mM $MgSO_4$, 10 mM KCl, 8 mM $(NH_4)_2SO_4$, and 1 mM $MnCl_2$. The reaction was performed on ice for 1 min followed by heat inactivation for 20 min at 70°C. The resulting products were analyzed on 1% agarose gel.

Step 2. Loop-1 linkers ligation. The partially digested products were ligated to individual loop-1 linkers (Sigma-Aldrich). These contained self-complementary sequences, which included recognition sequences for *EcoP15*I (CTGCTG) and *Fok*I (CATCC) (sequences are listed in Table 1). Ligations contained 2.5 μL partially digested DNA from step 1, 0.5 μL 10×Ligation Reaction Buffer (NEB), 1 μL (10 mM) loop-1 linker; 0.5 L 10 mM ATP (Sigma-Aldrich), and 0.5 μL T4 DNA Ligase (NEB); and were incubated at 16°C overnight.

Step 3. Single primer PCR (PCR-1). Loop-1 ligation products were then amplified using single primer PCR with the 5′BH1 primer (Sigma-Aldrich). PCR-1 amplification reactions contained 0.5 μL loop-1 linker ligation product, 2 μL single primer 5′BH1 (20 μM), 1 μL dNTP (10 mM, Sangon), 5 μL 10× PCR buffer [200 mM Tris-HCl (pH 8.4), 500 mM KCl, 15 mM $MgCl_2$], 0.5 μL Taq DNA polymerase (Clontech), and double-distilled water (ddH_2O) added to a final volume of 50 μL. Reactions were preheated at 95°C for 1 min, followed by 28 amplification cycles of 95°C for 15 s and 68°C for 1 min. PCR products were analyzed on 1% agarose gel. PCR-1 products were purified by extracting with two volumes of phenol:chloroform:isoamyl alcohol (25:24:1) (Sangon) and precipitated with 1/10 volume of 3 mol/L NaOAc (Sangon),

Table 1. Sequences of Linkers and Primers

Oligo name	*Sequence (5′-3′)*
19-bp Loop-1 linker	pCTTTTTTTCTGCTGCATCCCTGAACTGGGATCCGTTGGATGTGTACACATCCAA CGGATCCCAGTTCAGGGATGCAGCAGAAAAAAG
20-bp Loop-1 linker	pCTTTTTTCTGCTGGCATCCCTGAACTGGGATCCGTTGGATGTGTACACATCCAAC GGATCCCAGTTCAGGGATGCCAGCAGAAAAAG
21-bp Loop-1 linker	pCTTTTTCTGCTGGGCATCCCTGAACTGGGATCCGTTGGATGTGTACACATCCAAC GGATCCCAGTTCAGGGATGCCCAGCAGAAAAG
22-bp Loop-1 linker	pCTTTTCTGCTGGGGCATCCCTGAACTGGGATCCGTTGGATGTGTACACATCCAAC GGATCCCAGTTCAGGGATGCCCCAGCAGAAAG
23-bp Loop-1 linker	pTTTTCTGCTGGGGGCATCCCTGAACTGGGATCCGTTGGATGTGTACACATCCAAC GGATCCCAGTTCAGGGATGCCCCCAGCAGAAAA
Loop-2 linker	pCTTTTTGAGACCGACATCCCTCTGCAGACGATCCATCAGAGTCAGCTGACTCTGA TGGATCGTCTGCAGAGGGATGTCGGTCTCAAAAAG
5′BH1 primer	ACACATCCAACGGATCCCAGTTCAG
3′LG primer	GACTCTGATGGATCGTCTGCAGAG
5′U6 primer	AAGGTCGGGCAGGAAGAGGGC
3′H1 primer	TATTTGCATGTCGCTATGTGTTCT
NC sense	TTCTCCGAACGTGTCACGTTT
NC antisense	ACGTGACACGTTCGGAGAATT
HBV forward primer	TGTGGTTATCCTGCGTTAATG
HBV reverse primer	GCGTCAGCAAACACTTGG
MITF forward primer	CATCACCTTCAACAACAAC
MITF reverse primer	ATGCTCATACTGCTCCTC
BIRC5 forward primer	ACCGCATCTCTACATTCAAG
BIRC5 reverse primer	CAAGTCTGGCTCGTTCTC
GAPDH forward primer	GAAGGTGAAGGTCGGAGTC
GAPDH reverse primer	GAAGATGGTGATGGGATTTC

NC, negative control; p, phosphate; BIRC5, baculoviral IAP repeat-containing 5; GAPDH, glyceraldehyde 3-phosphate dehydrogenase; HBV, hepatitis B virus; MITF, microphthalmia-associated transcription factor.

1.5 μL Glycogen (20 mg/mL, Sangon), and 2.5 fold volumes of ice-cold ethanol (Sangon); samples were kept at −20 °C for 4 hrs, DNA pellets were collected by centrifugation and resuspended in 20 μL ddH_2O and stored at −20 °C.

Step 4. *EcoP15*I digestion. The PCR-1 products from the five (19-, 20-, 21-, 22-, and 23-bp) loop-1 linkers were mixed in equal quantities and then digested with *EcoP15*I (NEB). Ten microliters PCR-1 product mixtures were restricted in 100-μL reactions containing 10 μL 10×NEBuffer-3 (NEB); 10 μL ATP (10 mM, Sigma-Aldrich); 1 μL bovine serum albumin (BSA) (10 mg/mL, NEB); 10 μL *EcoP15*I (100 U, NEB); and 59 μL ddH_2O overnight at 37°C. *EcoP15*I digestion products were purified by phenol-chloroform extraction and alcohol precipitation as described above. DNA pellets were collected by centrifugation and resuspended in 11 μL ddH_2O.

Step 5. End-filling and loop-2 linker ligation. *EcoP15*I-generated sticky ends were end-filled with T4 DNA polymerase by adding 1.5 μL T4 DNA polymerase (4.5 U), 1.5 μL NEBuffer-2 (NEB), and 2 μL dNTP (1 mM, Sangon) to a total 15-μL reaction and incubated at 37°C for 15 min. Fragments of appropriate sizes (63-67 bp) were purified from 20% Tris-Borate-Ethylene Diamine Tetraacetic Acid (TBE) polyacrylamide gels using QIAEX II Gel Extraction Kit (Qiagen) and eluted with ddH_2O. The polyacrylamide gel electrophoresis (PAGE)–purified blunt-ended DNA fragments were ligated to a loop-2 linker containing a *Fok*I recognition sequence (CATCC). Next, 2.5 μL of DNA isolated by PAGE from step 4 was supplemented with 0.5 μL 10× ligation reaction buffer [500 mM Tris-HCl (pH 7.5, 25°C), 100 mM $MgCl_2$, 100 mM DTT, 25 μg/mL BSA]; 1 μL loop-2 linker (20 mM, Sigma-Aldrich); 0.5 μL ATP (10 mM, Sigma-Aldrich); 0.5 μL T4 DNA Ligase (NEB); and 0.5 μL ddH_2O. Reactions were incubated at 16°C overnight.

Step 6. PCR-2. Ligation products were diluted with 45 μL ddH_2O, and 0.5 μL of these used as templates for PCR-2 amplification. Reactions contained 0.5 μL diluted ligation products; 5 μL 10× PCR buffer [200 mM Tris-HCl (pH 8.4); 500 mM KCl; 15 mM $MgCl_2$]; 1 μL 3′LG primer (10 μM, Sigma-Aldrich); 1 μL 5′BH1 primer (10 μM, Sigma-Aldrich); 1 μL dNTP (10 mM, Sangon,); and 0.5 μL Taq DNA polymerase (Clontech) in a final volume of 50 μL. Reactions were preheated at 95°C for 1 min and amplified using 28 cycles of 95°C for 15 sec and 68°C for 1 min. After amplification, 10 μL of PCR products were analyzed on a 20% TBE polyacrylamide gel, and the remaining fragments purified using phenol–chloroform extraction and ethanol precipitation as described above; DNA pellets were resuspended in 20 μL ddH_2O.

Step 7. *Fok*I digestion. PCR-2 products were digested with *Fok*I enzyme; 50-μL reactions contained 20 μL purified PCR-2 products (from step 6), 2 μL *Fok*I (10 U, NEB), 5 μL NEBuffer-3 (NEB), and 23 μL ddH_2O, which was incubated at 37°C for 100 min. After digestion, 10 μL of products were analyzed on a 20% TBE polyacrylamide gel and appropriate bands purified by PAGE as described above.

Step 8. Cloning to RNAi expression vector. *Fok*I-digested fragments were ligated into linearized pRNAi-U6H1/Neo. pRNAi-U6H1/Neo was digested with *BsmB*I and dephosphorylated with calf intestinal alkaline phosphatase according to manufacturer's (NEB) protocols. One hundred nanogram vectors were ligated to 2 μL gel-purified *Fok*I digested insert DNA from step 7 using T4 DNA ligase according to the manufacturer's protocol (NEB). Ligations were purified by ethanol precipitation and then electrotransformed into MegaX DH10B™ Cell (Invitrogen) using a MicroPulser (Bio-Rad) according to the manufacturer's protocols and transformed colonies selected with Kanamycin.

Preparation of pRNAi-U6H1/Neo

The pRNAi-U6H1/Neo vector was modified from pDsi-PHER-GFP vector (MoleculA). An insert DNA fragment was synthesized (Biomics), this contained the human U6 and H1 promoter sequences, two inversely oriented *BsmB*I restriction sites, and an *Sfi*I site: these sequences were flanked by *Hind*III or *Mlu*I sites and were cloned into *Hind*III/*Mlu*I digested pDsiPHER-GFP. The sequence of the fragment was:
5′-AAGCTTCTCGAGGAATTCAAGGTCGGGCAGGAAG
AGGGCCTATTTCCCATGATTCCTTCATATTTGCATA
TACGATACAAGGCTGTTAGAGAGATAATTAGAATT
AATTTGACTGTAAACACAAAGATATTAGTACAAAA
TACGTGACGTAGAAAGTAATAATTTCTTGGGTAGTT
TGCAGTTTTAAAATTATGTTTTAAAATGGACTATCA
TATGCTTACCGTAACTTGAAAGTATTTCGATTTCTTG
GGTTTATATATCTTGTGGAAAGGACGAAAAAAGAG
ACGGCCGTGTTGGCCGTCTCTTTTTTGAGTGGTCTCA
TACAGAACTTATAAGATTCCCAAATCCAAAGACATT
TCACGTTTATGGTGATTTCCCAGAACACATAGCGAC
ATGCAAATATCTCGAGACGCGT-3′.

Validation of cloning efficiency in SURER library

To analyze SURER libraries, bacterial colonies were randomly picked and inoculated into 400 μL Lysogeny broth medium [1% (w/v) tryptone, 0.5% (w/v) yeast extract, 1% (w/v) NaCl, pH 7.0] in 48-well plates. Cultures were incubated at 37°C with a continuous shaking for 2 h at 220 rpm. Cultures were screened with PCR by 5′U6 primer and 3′H1 primer (Invitrogen). Reactions contained 2 μL cultured bacteria, 0.5 μL 5′U6 primer (10 μM), 0.5 μL 3′H1 primer (10 μM), 0.5 μL dNTP (10 mM, Sangon), 3 μL 10× PCR buffer [200 mM Tris-HCl (pH 8.4), 500 mM KCl, 15 mM $MgCl_2$], 0.3 μL Taq DNA polymerase (Clontech), and ddH_2O to a final volume of 30 μL. Reactions were preheated at 95°C for 5 min and amplified for 25 cycles at 95°C for 15 s, 62°C for 30 s, and 72°C for 40 s, then held at 72°C for 7 min for final extension. Five microliters of each PCR product were analyzed on 1% agarose gel. *Sfi*I digestion was used to define clones containing inserts; 4 μL of the above PCR reactions were digested with *Sfi*I according to the manufacturer's protocol (NEB). Products were analyzed on 1% agarose gel, and plasmids of validated clones prepared using Plasmid Mini Kit (Qiagen) and sequenced with 5′U6 or 3′H1 primer.

sRNA expression cassettes preparation

Short RNA expression cassettes for cell transfection were prepared using PCR with 5′U6 and 3′H1 primers. The PCR reaction contained 1 μL plasmid of sRNA clone (10 ng), 1 μL

5′U6 primer (10 μM), 1 μL 3′H1 primer (10 μM), 1 μL dNTP (10 mM, Sangon), 5 μL 10×PCR buffer [200 mM Tris-HCl (pH 8.4), 500 mM KCl, 15 mM $MgCl_2$], 0.5 μL Taq DNA polymerase (Clontech), and ddH_2O to a final volume of 50 μL. Reactions were preheated at 95°C for 5 min and amplified for 25 cycles of 95°C for 15 s, 62°C for 30 s, and 72°C for 40 s, then held at 72°C for 7 min for final extension. Two microliters of each PCR product was analyzed on 1% agarose gel.

As a negative control (NC), 100 μM NC sense and antisense strand (Table1, Biomics) were annealed by using 95°C heating for 10 min and cooled to room temperature. Two microliters of annealed oligos were cloned into linearized, phosphorylated pRNAi-U6H1/Neo as described above. Reactions were purified and transformed into *Escherichia coli* (*E. coli*), plasmids were sequenced as described above, and an appropriate clone was selected.

Cell culture and transfection

Human HepG2 2.2.15, A431, and HepG2 cell lines (Biomics) were used to assay silencing. Cells were cultured in Dulbecco's modified Eagle's medium supplemented with 10% fetal bovine serum (Gibco) and incubated at 37°C in 5% CO_2. One hundred thousand cells per well were seeded 24 h before transfection into 96-well plates at 70%–80% confluence. Transfection of 100 ng sRNA expression cassettes and 50 nM chemical synthesized sRNAs were conducted with Lipofectamine® 2000 (Invitrogen) according to the manufacture's recommendations.

Real-time quantitative PCR analysis

The levels of mRNAs encoding HBV DNA polymerase, MIF, and BIRC5 were determined by real-time qantitative PCR (RT-qPCR). At 48 h post-transfection, mRNAs were extracted using TurboCapture mRNA Kit (Qiagen) using the manufacturer's protocol and used as templates for RT-qPCR reactions. The primers used to detect HBV, MITF, and BIRC5 as shown in Table 1. Target mRNA levels were normalized to glyceraldehyde phosphate dehydrogenase (GAPDH) mRNA levels. Triplicate RT-qPCR reactions were analyzed for each mRNA sample. The 25-μL RT-qPCR reactions contained 4 μL template RNA (50 ng), 12.5 μL of 2× SensiMix One-Step (Quantance), 1 μL forward and reverse primers (10 μM, Biomics), 0.5 μL 50× SYBR Green I (Quantance), and RNase-free water to 25 μL. Reverse transcription was at 42°C for 30 min; reactions were then preheated at 95°C for 7 min, followed by 45 amplification cycles, which involved denaturation at 95°C for 20 sec, annealing at 60°C for 30 sec, and extension at 72°C for 30 sec.

Three siRNAs—c-2, c-38, and c-42—were synthesized; their sequences were based on the sequences of clones 2, 38, and 42 from the BIRC5 SURER library. These were transfected into HepG2 cell line and mRNAs extracted for the RT-qPCR method described above; the NC sRNA (sense: UUCUCCGAACGUGUCACGUdTdT; antisense: ACGUGA CACGUUCGGAGAAdTdT) was used negative control.

Western blot analysis

HepG2 cells were plated at a concentration of 1×10^6 cells per well in 6-well plates and grown for 24 h until they reached 70%–80% confluence then transfected with sRNAs c-2, c-38, and c-42. Cells were harvested 48 h after transfection lysed in ice-cold cell M-PER Mammalian Protein Extraction Reagent (Pierce), and proteins separated on SDS-PAGE and transferred to polyvinylidene fluoride membranes (Millipore). To detect BIRC5, filters were probed with a polyclonal rabbit anti-human BIRC5 (Abcam) followed by goat anti-rabbit immunoglobin G–horseradish peroxidase (IgG-HRP) (Santa Cruz). β-actin levels were used for controls and were determined using mouse anti-hunan β-actin (Santa Cruz) followed by goat anti-mouse IgG-HRP (Santa Cruz). Proteins were visualized by chemiluminescence with ECL (Promega). The relative amount of proteins on the blots was determined by Image J software (National Institutes of Health).

Cell proliferation assay

HepG2 cell proliferation was measured by Cell Counting Kit-8 (CCK-8) detection kit (Dojindo). Cells were plated at a concentration of 5×10^3 cells per well in 96-well plates. At 24 h, 48 h, 72 h, and 96 h after siRNA transfection, CCK-8 solution was applied followed by 2 h incubation at 37°C. Absorbance values of all wells were then determined at 490 nm in Microplate Reader (Bio-Rad).

Statistical analysis

All experiments were performed independently three times, the results were shown as mean ± standard deviation, and statistical analyses were performed using SPSS19.0 software. The differences between groups were compared using Student's t-test to assess statistical significance. All P values were based on a two-sided statistical analysis, and $P<0.05$ was considered to indicate statistical significance.

Results

SURER library preparation

SURER library construction is shown diagrammatically in Fig. 1, a detailed protocol is described in ''Materials and Methods,'' and primers used to construct libraries are listed in Table 1. First, double-stranded DNAs (dsDNAs) were randomly and partially digested to produce100- to 300-bp fragments by *DNase*I in the presence of Mn^{2+} ions [33] (Fig. 1, Step 1). The fragments were then ligated to individual loop-1 linkers (Fig. 2A), which contained the recognition sequences of *EcoP*15I and *Fok*I adjacent to a universal PCR anchor sequence (Fig. 1, Step 2). As shown in detail in Fig. 2A, five different loop-1 linkers were used to generate independent pools of 19-, 20-, 21-, 22-, and 23-bp cDNA inserts. *EcoP15*I cleaves 25–27 bp outside of its recognition site, thus adjusting the number of the poly A/T sequence between the *EcoP15*I recognition site in loop-1 linker(s) and cDNA fragments, specifying the size of restriction fragments (e.g. 19–23 bp) generated by this protocol. Single loop-1 linkers can be used if a distinct length of sRNA is required.

Efficient cleavage of dsDNAs by *EcoP15*I requires the presence of two inversely oriented restriction sites with head-to-head orientations [34]. After blunt-end ligation of loop-1 linker(s) to dsDNAs, a single primer PCR (PCR-1) was performed (Fig. 1, Step 3) for each linker ligation; these were then pooled for subsequent steps.

*EcoP15*I digestion was carried out after PCR-1 (Fig. 1, Step 4) to generate 19- to 23-bp fragments derived from the

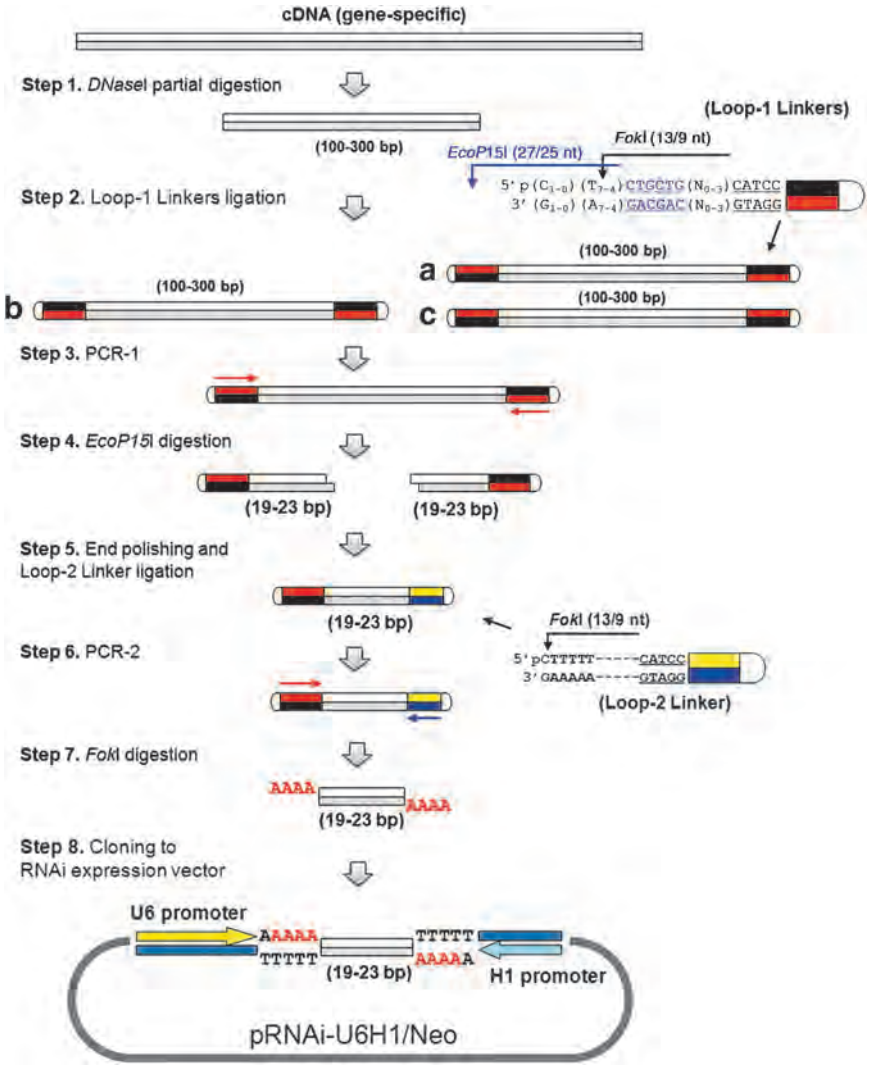

FIG. 1. General scheme for SURER (size unbiased representative enzymatically generated RNA interference [RNAi]) library construction. *Step 1:* Partial *DNase*I digestion of gene-specific complementary DNAs (cDNAs) to produce 100- to 300-bp fragments. *Step 2:* Three kinds of molecules (-a, -b, and -c) with different linker orientations are generated after loop-1 linker ligation. Only molecule-a can be digested by *EcoP15*I since the enzyme requires the presence of two inversely oriented recognition sites for efficient cleavage. The loop-1 linker contains the recognition sites of *EcoP15*I (to generate fragments of appropriate size) and *Fok*I (for cloning into an expression vector). *Step 3:* Single primer polymerase chain reaction (PCR) amplification (PCR-1). *Step 4:* *EcoP15*I digestion, which generates 19- to 23-bp small RNA (sRNA) encoding fragments from PCR-1 amplified fragments. *Step 5:* End-filling by T4 DNA polymerase followed by loop-2 linker ligation. *Step 6:* Double primers PCR amplification (PCR-2) to amplify appropriate fragments. *Step 7:* *Fok*I digestion to generate sRNA fragments. *Step 8*: Cloning into linearized pRNAi-U6H1/Neo.

original cDNA. The loop-1 linkers contained sites for both *EcoP15*I and a type-2 restriction site, *Fok*I, adjacent to a PCR anchor sequence (Fig. 2A). *EcoP15*I cleaves 25–27 bp outside of their recognition sequences, thus adjusting the number of the poly ''A/T'' sequence between the *EcoP15*I recognition site in loop-1 linker(s) and cDNA fragments, specifying the size of restriction fragments (e.g. 19–23 bp) generated by this protocol.

*EcoP15*I cleavage leaves two base-pair 5′ overhangs; these were then end-filled using T4 DNA polymerase in the presence of dNTPs [35] (Fig. 1, Step 5). After gel purification, the blunt-ended DNAs were ligated to the loop-2 linker (Fig. 2B). These ligation products were then used as templates for the second PCR amplification (PCR-2; Fig. 1, Step 6). The loop-2 linker creates a PCR anchor and specifies *Fok*I restriction sites for subsequent cloning of amplified fragments. *Fok*I cleavage of PCR-2 amplified products generates 4-nt 5′ overhangs of amplified fragments, in this instance 5′ with AAAA overhangs at each end (Fig. 1, Step 7).

The *Fok*I digested products were then cloned into the RNAi expression vector pRNAi-U6H1/Neo (Fig. 1, Step 8). A map of this is shown in Fig. 3, it contains two opposing polymerase III (pol III) promoters (U6 and H1) separated by a polylinker. The polylinker contains two *BsmB*I sites, cleavage of which generated cloning vectors with TTTT 3′ overhangs, compatible with the *Fok*I digested PCR-2 products (Fig.1, Step 7). These poly T and poly A tracts act as pol III transcriptional terminators. The polylinker also contains a *Sfi*I restriction site, loss of which can be conveniently used to screen colonies for recombinant molecules.

Ligations were transformed into *E.coli*, to generate pools of recombinants containing fragments of cDNAs expected to range from 19 to 23 bp. Resultant colonies were screened with PCR by 5′U6 and 3′H1 primers (Table 1) and clones lacking the diagnostic *Sfi*I restriction site were sequenced to characterize libraries.

SURER library from cDNA encoding DNA polymerase of Hepatitis B virus

A full-length cDNA of HBV DNA polymerase (NCBI Accession No. U95551) CDS was synthesized as two fragments of 1625 bp and 874 bp (Fig. 4A). DNA was randomly and partially digested to generate blunt-ended fragments using *DNase*I. The preferable length for library construction was about 100–300 bp (Fig. 4B).

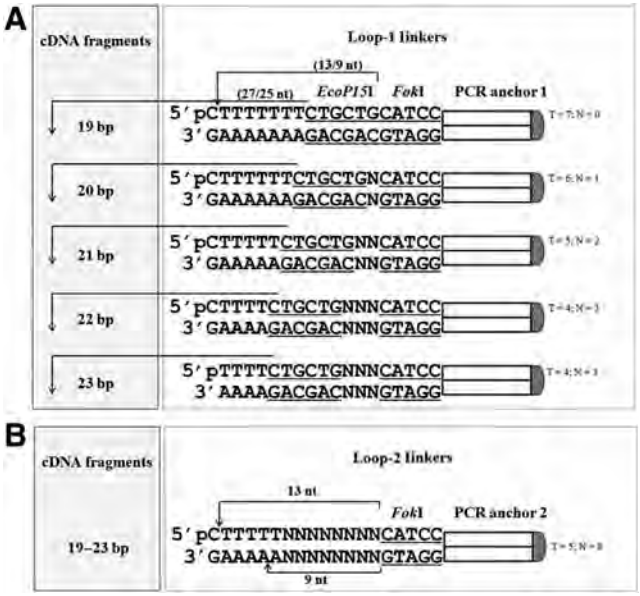

FIG. 2. **(A)** Structures of loop-1 linkers (19–23 bp). Self-annealed loop-1 linkers contained *EcoP15*I (CTGCTG) and *Fok*I (CATCC) sites followed by a universal PCR anchor. Different lengths of sRNAs can be generated by shifting the number of T/A pairs between the *EcoP15*I site and cDNA sequences. The function of ''N'' (which can be A, T, C, or G) between the *EcoP15*I and *Fok*I recognition sites is to maintain cloning sites (AAAA overhangs) after *Fok*I digestion, which allows TA cloning and can also act as RNA transcription stop (TTTTT) sites (Fig. 1). No ''junk'' sequences arise from this cloning strategy. **(B)** Structures of loop-2 linker. Self-annealed loop-2 linker contained a *Fok*I (CATCC) site followed by a universal PCR anchor 2.

Individual loop-1 linkers were ligated to the blunt-ended DNAs by T4 DNA ligase and ligation products subject to single primer PCR amplification (Fig. 4C). Following this step, individual products were pooled and fragments digested with *EcoP15*I to produce sticky-ended DNA molecules with two nucleotide 5′ overhangs, which were then end-filled using T4 DNA polymerase in the presence of dNTPs. Products were purified as 63- to 67-bp fragments by PAGE with Novex® 20% Tris-Glycine Mini Gels (Invitrogen), as shown in Fig. 4D. After gel purification, the loop-2 linker (Fig. 2B) was ligated to the blunt-ended DNA using T4 DNA ligase. The ligation products were then PCR amplified (PCR-2) by 5′BH1 and 3′LG primers (Table 1), as shown in Fig. 4E. After gel purification of PCR-2 products, which ranged from 108 to 112 bp, fragments were digested with *Fok*I; resultant products ranged from 29 to 32 bp as shown in Fig. 4F. The *Fok*I digested products were then cloned into linearized pRNAi-H1U6/Neo vector. Libraries were characterized by colony PCR and *Sfi*I digestion and selected clones sequenced.

Small RNA distribution profiles of randomly selected colonies from the SURER library

SURER libraries were prepared using cDNA templates of the HBV DNA polymerase CDS (2499 bp, Accession No. U95551), a conserved domain of MITF (1210 bp, Accession No. NM_198159) and the CDS of BIRC5 gene (429 bp, Accession No. NM_001168). Positive clones were randomly selected for sequencing, and insert sequences were aligned with cDNA sequence of target genes. As shown in Fig. 5, sRNA clones were randomly distributed throughout the sequences of all templates. Moreover, most clones were from 19 to 23 bp (Fig. 5).

Gene silencing profiles of randomly selected sRNA clones from the SURER Library

To define the silencing activity of clones, sRNA expression cassettes from the HBV, MITF and BIRC5 SURER libraries were PCR amplified using the 5′U6 and 3′H1 primers (Table 1). These were transfected into HepG2 2.2.15, A431, and HepG2 cells respectively, using Lipofectamine® 2000. At 48 h post-transfection, mRNAs were isolated from cells for RT-qPCR determination of mRNA levels using gene specific primers (Table 1). Results were analyzed by $2^{-\Delta\Delta Ct}$ method [36]; GAPDH was used as the reference gene.

Large scale screening (507 unique sRNA clones) was performed in vitro to assay for silencing of HBV polymerase mRNA. 100 sRNA clones silenced HBV polymerase by

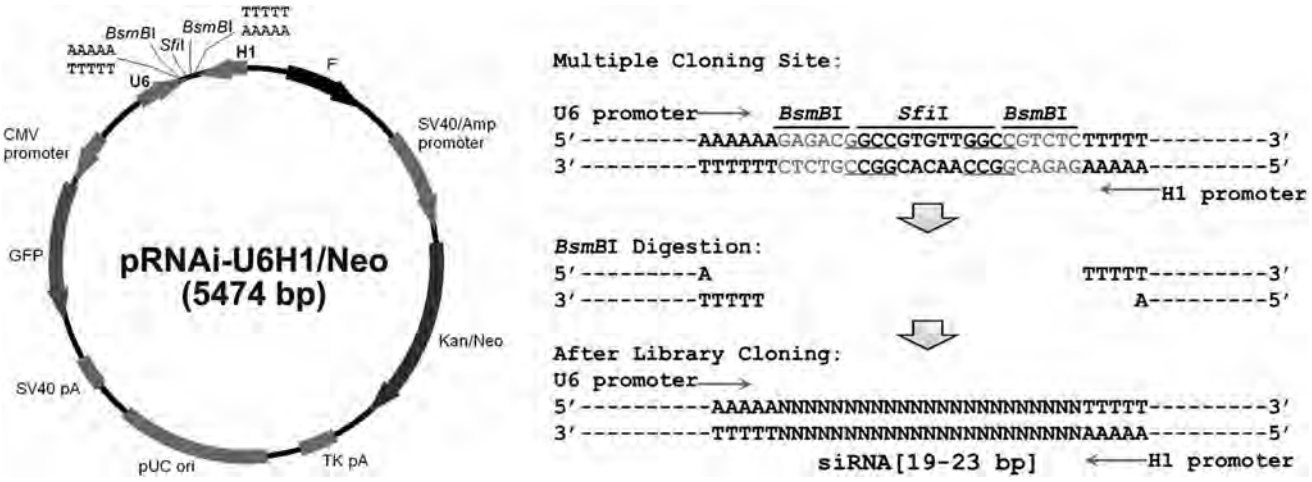

FIG. 3. Schematic diagram of the RNA interference expression vector pRNAi-U6H1/Neo. The vector contains a multiple cloning sites with two *BsmB*I restriction sites to permit cloning of *Fok*I-digested sRNA fragments and an *Sfi*I site to assist in screening for recombinants.

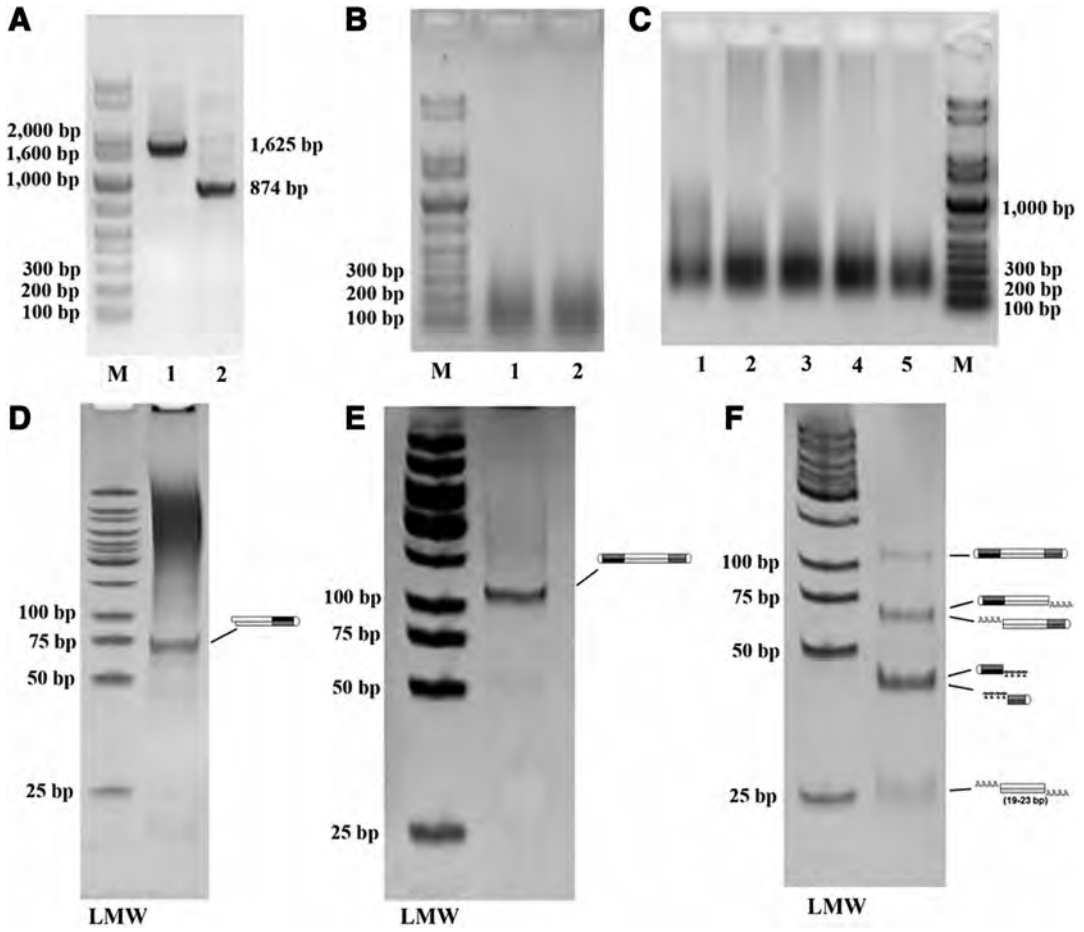

FIG. 4. Gel electrophoretic analysis showing steps in preparation of SURER library from HBV DNA polymerase cDNA. **(A)** The full-length cDNA of HBV DNA polymerase of was synthesized as two fragments of 1625 bp (*1*) and 874 bp (*2*). **(B)** Partial digestion of 1625 bp (*1*) and 874 bp (*2*) target DNAs with *DNase*I generated fragments ranging from 100 to 300 bp. **(C)** Single primer PCR amplification (PCR-1) to generate appropriate substrates for library preparation. Substrates for these reactions were ligations using the 19-bp loop-1 linker (*1*); 20-bp loop-1 linker (*2*); 21-bp loop-1 linker (*3*); 22-bp loop-1 linker (*4*); or 23-bp loop-1 linker (*5*). **(D)** *EcoP15*I cleavage of pooled PCR-1 fragments. **(E)** PCR-2 amplification using 5′BH1 and 3′LG primers. **(F)** *Fok*I digestion of PCR-2 amplified products. Diagrammatic representations of products are shown to the *right*. M, 1kb plus DNA ladder (Invitrogen); LMW, low molecular weight DNA ladder (NEB).

≥50%, 16 of which resulted in ≥70% knockdown efficiency (Fig. 6A). Sixty-three sRNA clones from the MITF SURER library were screened for activity; 32 sRNAs were effective in silencing MITF by ≥50%, 14 of these resulted in ≥70% knockdown efficiency (Fig. 6B). Twenty-six sRNA clones from the BIRC5 SURER library were screened for activity; 13 sRNAs were effective in silencing BIRC5 by ≥50%, 4 of these resulted in ≥70% knockdown efficiency (Fig. 6C).

To confirm the activity of BIRC clones, three siRNAs were chemically synthesized based on the sequences of clones 2, 38, and 42 (c-2, c-38, c-42) and assayed for knockdown of the endogenous BIRC5 gene in HepG2 cells, and the three designed [37] and synthetic siRNAs (s-1, s-2, s-3) used for comparison. Levels of BIRC5 mRNA and protein were determined in siRNA treated cells 48 h after transfection using RT-qPCR and western blots. The result of RT-qPCR showed that the knockdown efficiencies of designed siRNAs were all lower than 50%, not stronger than screened siRNAs (>80%) (Fig. 7A). Furthermore, BIRC5 protein was strongly reduced in HepG2 cells treated with c-2, c-38, and c-42 compared with negative control (c-NC) treated and untransfected cells (Fig. 7B). Silencing of BIRC5 was expected to inhibit cell proliferation in siRNA transfected cells. CCK-8 assays in cells transfected with c-2, c-38, and c-42 demonstrated reduced signals at 48 h, 72 h, and 96 h post-transfection compared with c-NC treated and untransfected cells (Fig. 7C), indicating reduced proliferation.

Discussion

The SURER library protocol has several advantages over alternative methods. Importantly the lengths of sRNAs expressed from SURER libraries are representatively distributed from 19 to 23 bp, as a consequence of using different loop-1 linkers. In addition, the SURER cloning strategy does not result in incorporation of additional sequences, such as linkers, into clones. Moreover, the PCR amplification steps incorporated into the library construction process do not seem to appreciably bias clone representation (Fig. 5) and also ensures adequate materials are available for the various steps in the protocol.

The representative sRNA size distribution from 19 to 23 bp in all SURER libraries was achieved using five rationally

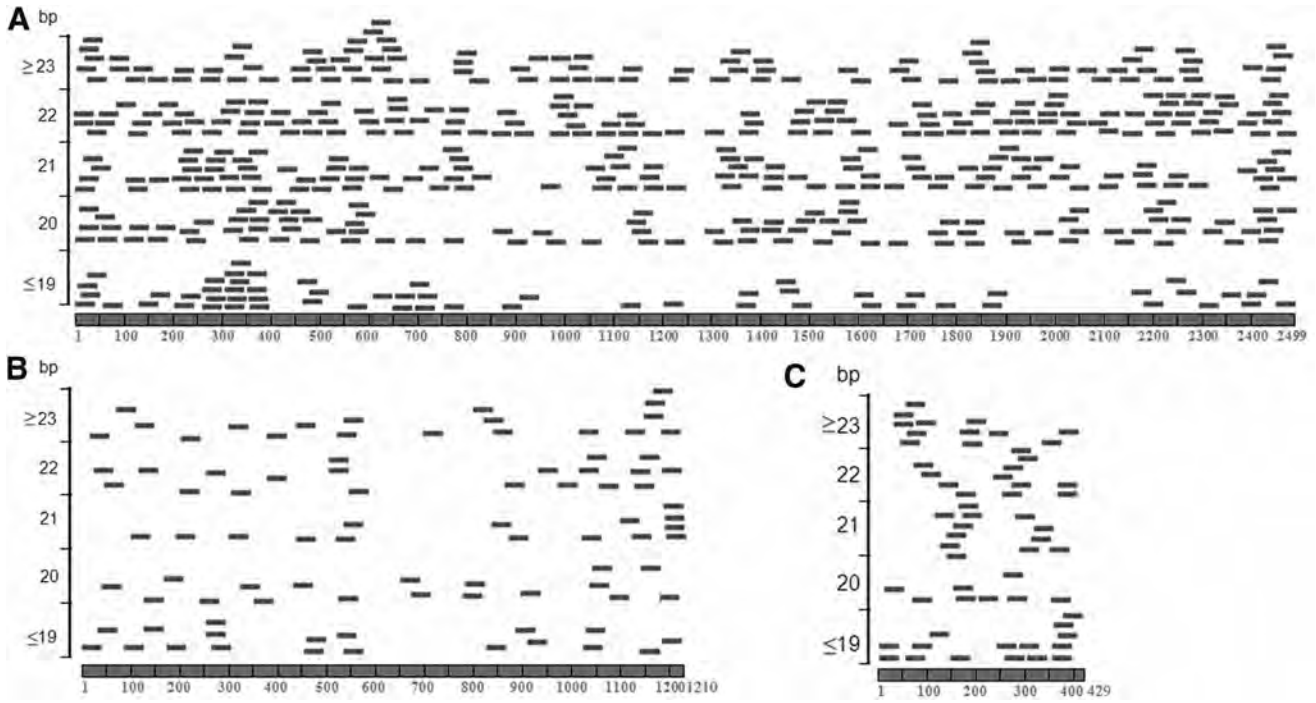

FIG. 5. Site and size distribution profiles of clones randomly selected from HBV, MITF, and BIRC5 SURER libraries. The *x*-axis represents cDNA sequences; sequences of sRNA-expressing clones are aligned above these. The *y*-axis denotes the size of sRNA clones (≤ 19, 20, 21, 22 and ≥ 23). **(A)** 604 clones from HBV DNA polymerase SURER library. **(B)** 120 clones from MITF conserved domain SURER library. **(C)** 59 clones from BIRC5 SURER library.

designed loop-1 linkers (Fig. 2A) where the size of the resulting cDNA fragments is controlled by the number of A nucleotide (nt) between cDNA fragments and the *EcoP15*I site sites in Loop-1 linkers used for library construction (Fig. 1). To meet our internal RNAi therapeutic screening purpose, steps 2 and 3 were performed with each individual loop-1 primers and analyzed on 1% agarose gel (Fig. 4C); samples were then pooled for subsequent manipulations. The clones we analyzed showed the expected size distribution, similar to the natural length (19–23 bp) of sRNAs generated by Dicer processing in living cells [38,39]. Moreover, clones of the different size classes seemed to be randomly distributed across the cDNA sequences used to prepare the SURER libraries (Fig. 5). The five different sizes cover almost all sites of a target gene which is determined by the initial *DNase*I partial digestion (Fig. 1) as previously described [24,28,40,41]. However, we did find some sizes were outside of this range $< 5\%$ clones gave sizes > 23 bp and < 19 bp, respectively. We suspect *EcoP15*I, a type-3 restriction/modification enzyme, does not always cleave precisely at 25–27 bp from its recognition site. This phenomenon has also been observed when using *Mme*I (18–20 bp) for library preparation enzymatically [26].

*Fok*I restriction sites were incorporated into both the loop-1 and loop-2 linkers to generate TTTTT cohesive ends, which permits cloning into *BsmB*I-digested pRNAi-U6H1/Neo, these sequences also act as pol III transcriptional terminators. The loop-1 linkers contain additional bases (Ns in Fig. 2A) which maintained appropriate spacing between the *Fok*I sites and the A/T regions to ensure an appropriate AAAA overhang is generated. The cloning efficiency for SURER libraries reached $\sim 3 \times 10^5$ colony-forming units (~ 2.5 μg final cDNA was used for vector ligation), with a $> 90\%$ recombination rate (data not shown). Given a gene is 3 kb in length, a gene-specific library with a $\sim 3 \times 10^5$ independent clones is large enough to cover each sRNA site for a gene targeted. In this study, the three SURER libraries were successfully constructed from the templates of full-length cDNA (HBV DNA polymerase and BIRC5) or a domain of MITF gene. The length of the starting templates ranged from 429 (BIRC5) to 2499 bp (HBV DNA polymerase). As shown in Fig. 5, the distribution of sRNAs in these libraries is quite representative, particularly for the HBV polymerase, where larger numbers of clones were analyzed, where more than 80% of sRNA clones were non-overlapping recombinants (data not shown).

The SURER protocol involves two PCR steps. The first (Fig. 1, Step 3) is a single primer PCR, which is used to specifically amplify substrates containing opposing *BsmB*I sites present in the loop-1 primers (Fig. 1, Step 2). The second (Fig. 1, Step 6) is a conventional PCR used to specifically amplify molecules containing both loop-1 and loop-2 primers, which are required for cloning into the expression cassette. The three SURER libraries described here show excellent coverage of the target genes, indicating these steps had not significantly biased representation. The protocol does not involve amplification of palindromes another potential source of bias [28].

Constructs specifying potent knockdown for three targets (HBV, MITF, and BIRC5) were defined by screening SURER libraries. For HBV, 19.8% (100/507) of HBV SURER library clones gave $\geq 50\%$ gene knockdown, 3.2% of clones showed $\geq 70\%$ gene knockdown (Fig. 8), none of these have been previously described. We have developed siRNAs and ddRNAi constructs based on these sequences, which also

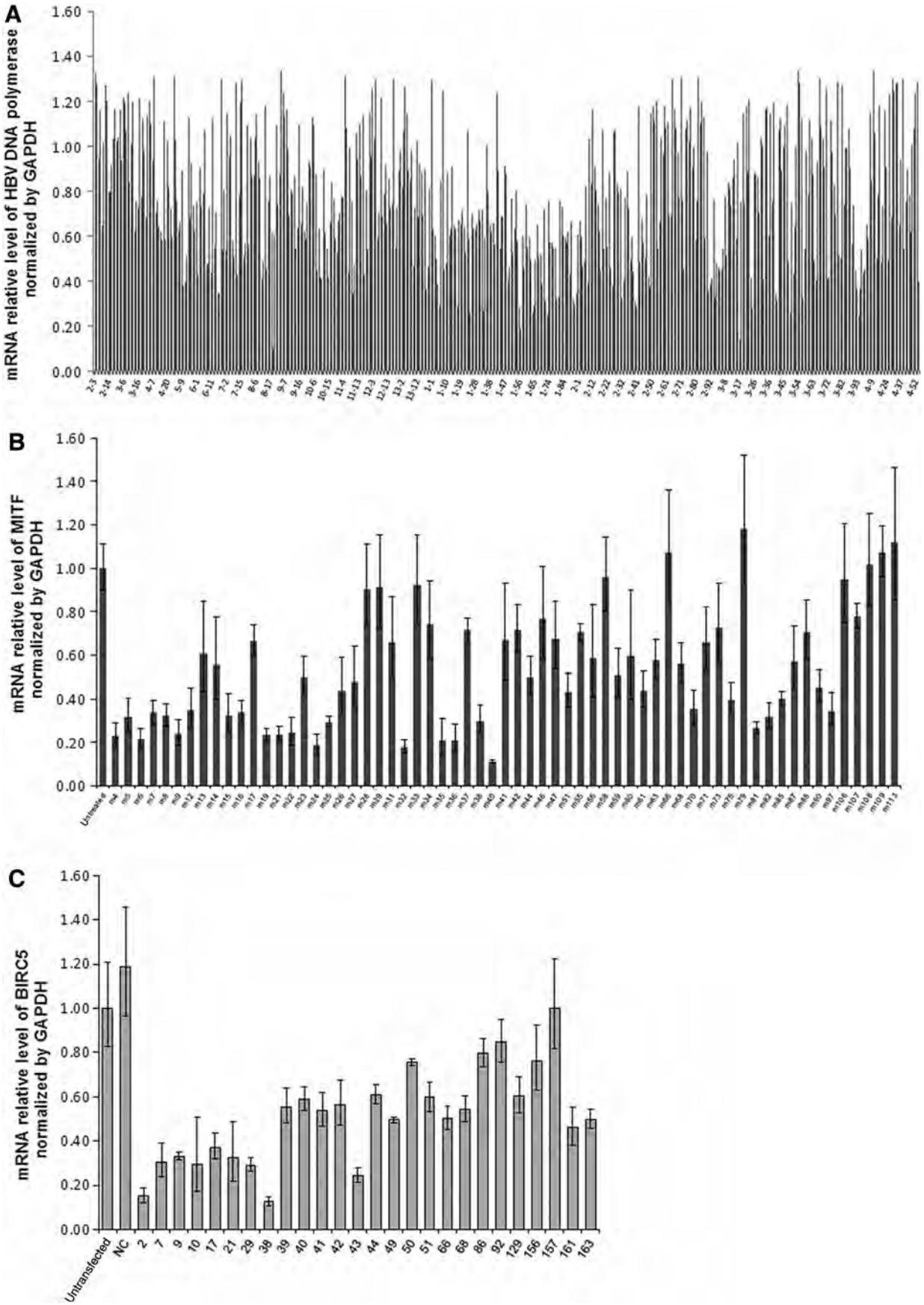

FIG. 6. Gene silencing efficiency of SURER clones determined using real-time quantitative PCR (RT-qPCR), normalized to GAPDH. **(A)** Relative levels of HBV polymerase mRNA in HepG2 2.2.15 cells treated with different sRNA expression cassettes selected from SURER library. **(B)** Relative mRNA levels of MITF in A431 cells treated with different sRNA expression cassettes. **(C)** Relative mRNA levels of BIRC5 in HepG2 cells treated with different sRNA expression cassettes.

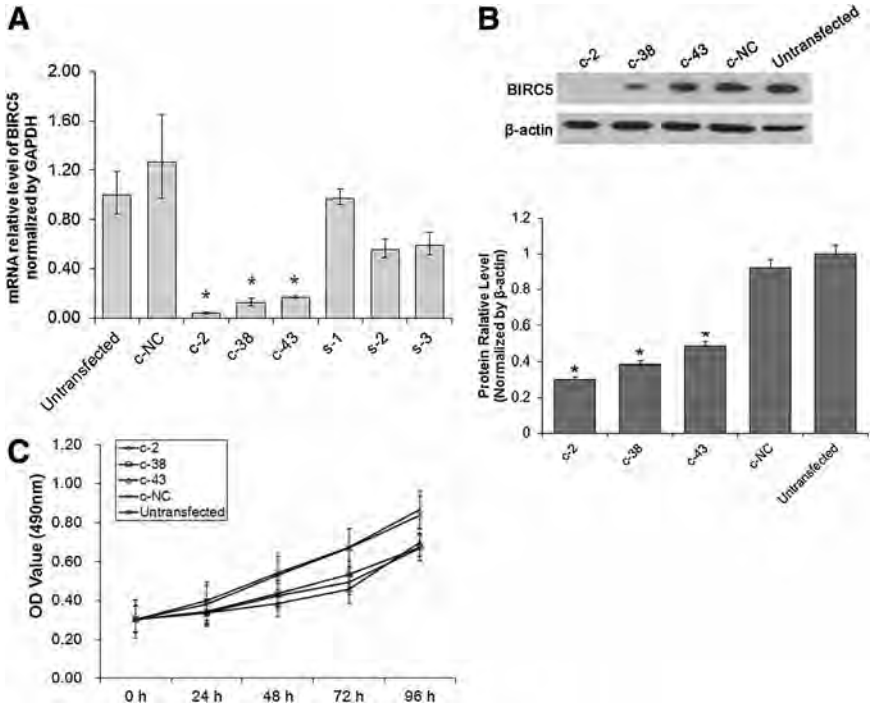

FIG. 7. Knockdown of BIRC5 with small interfering RNAs (siRNAs) defined by SURER screen. **(A)** Relative levels of BIRC5 mRNA in HepG2 cells treated with siRNAs: c-2, c-38, and c-43 were determined using RT-qPCR and normalized to levels of GAPDH mRNA, the three designed and synthetic siRNAs (s-1, s-2, s-3) used for comparison. **(B)** Relative protein levels of BIRC5 in cells treated with the indicated siRNAs were determined by western blots and normalized to levels of β-actin. **(C)** Cell proliferation in BIRC5 siRNA-treated cells was analyzed using CCK-8 assays. Growth curve of cells is shown for each treatment at 0, 24, 48, 72, and 96 hours. Values were given as mean ± SD of three separate experiments with triplicate wells per condition. $*P < 0.05$.

showed strong silencing activity (data not shown). For MITF, 50.8% (32/63) of clones gave ≥50% gene knockdown, and 22.2% of clones showed ≥70% gene knockdown (Fig. 8). For BIRC5, three clones (2, 38, 42) showed 80%–90% knockdown of mRNA (Fig. 6C). sRNAs were synthesized based on the sequences of these and potent knockdown confirmed at the level of mRNA, protein, and biological activity (Fig. 7). Only a small region (429 bp) of the BIRC5 gene screened, which was too short to be designed and found siRNAs with high knockdown efficiency using existing computer algorithms [37,42–43]. Screening SURER libraries overcomes the shortcomings of computer design algorithms.

In summary, we provide an innovative library construction method for RNAi screens. The SURER library construction protocol can be readily expanded to other kind of small RNA libraries such as miRNA and saRNA libraries where RNAs in the range of 19 to 23 bp show biological activity. Sequences derived from all or parts of open reading frames (ORFs), 5′ or 3′UTRs or promoter regions of target sequences can be readily screened. Incorporation of the pRNAi-U6H1/Neo expression cassette into new vectors might further increase the potential of the SURER strategy. The SURER library opens new ways for RNAi therapeutic screens in a fast and simple manner.

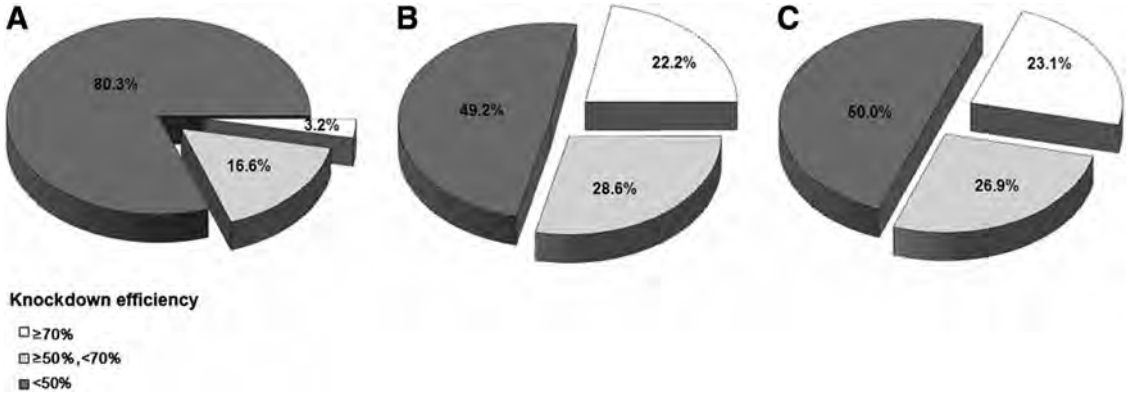

FIG. 8. Knockdown efficiency in three different SURER libraries. **(A)** 19.8% of sRNA clones silenced HBV polymerase by ≥50%, 3.2% of which resulted in ≥70% knockdown efficiency. **(B)** 50.8% of sRNAs were effective in silencing MITF by ≥50%, and 22.2% of these resulted in ≥70% knockdown efficiency from the MITF SURER library. **(C)** 50% of sRNAs were effective in silencing BIRC5 by ≥50%, and 23.1% of these resulted in ≥70% knockdown efficiency from the BIRC5 SURER library.

Acknowledgments

This work was supported National Science and Technology Major Project from National Natural Science Foundation of China (2011ZX09401-012); National High Technology Research and Development Program of China (863 Program, 2012AA022501). The HBV work was financially supported by Benitec Biopharma Ltd.

Author Disclosure Statement

No competing financial interests exist.

References

1. Fire A, Xu S, Montgomery MK, Kostas SA, Driver SE and Mello CC. (1998). Potent and specific genetic interference by double-stranded RNA in Caenorhabditis elegans. Nature 391:806–811.
2. Hannon GJ. (2002). RNA interference. Nature 418:244–251.
3. Martinez J, Patkaniowska A, Urlaub H, Lührmann R and Tuschl T. (2002). Single-stranded antisense siRNAs guide target RNA cleavage in RNAi. Cell 110:563–574.
4. Li T, Wu M, Zhu YY, Chen J and Chen L. (2014). Development of RNA interference-based therapeutics and application of multi-target small interfering RNAs. Nucleic Acid Ther 24:302–312.
5. Buchholz F, Kittler R, Slabicki M and Theis M. (2006). Enzymatically prepared RNAi libraries. Nat Methods 3:696–700.
6. Strezoska Ž, Licon A, Haimes J, Spayd KJ, Patel KM, Sullivan K, Jastrzebski K, Simpson KJ, Leake D, van Brabant Smith A and Vermeulen A. (2012). Optimized PCR conditions and increased shRNA fold representation improve reproducibility of pooled shRNA screens. PLoS One 7:e42341.
7. Tan H, Fan J, Bao J, Dy JG and Zhou X. (2012). A computational model for compressed sensing RNAi cellular screening. BMC Bioinformatics 13:337.
8. Kawasaki H, Suyama E, Iyo M and Taira K. (2003). siRNAs generated by recombinant human Dicer induce specific and significant but target site-independent gene silencing in human cells. Nucleic Acids Res 31:981–987.
9. Watanabe T, Totoki Y, Toyoda A, Kaneda M, Kuramochi-Miyagawa S, Obata Y, Chiba H, Kohara Y, Kono T, et al. (2008). Endogenous siRNAs from naturally formed dsRNAs regulate transcripts in mouse oocytes. Nature 453:539–543.
10. Yang D, Goga A and Bishop JM. (2004). RNA interference (RNAi) with RNase III prepared siRNAs. Methods Mol Biol 252:471–482.
11. Allen E, Xie Z, Gustafson AM and Carrington JC. (2005). microRNA-directed phasing during trans-acting siRNA biogenesis in plants. Cell 121:207–221.
12. Corrêa RL, Steiner FA, Berezikov E and Ketting RF. (2010). MicroRNA-directed siRNA biogenesis in Caenorhabditis elegans. PLoS Genet 6:e1000903.
13. Dalakouras A, Moser M, Zwiebel M, Krczal G, Hell R and Wassenegger M. (2009). A hairpin RNA construct residing in an intron efficiently triggered RNA-directed DNA methylation in tobacco. Plant J 60:840–851.
14. Qi X, Bao FS and Xie Z. (2009). Small RNA deep sequencing reveals role for Arabidopsis thaliana RNA-dependent RNA polymerases in viral siRNA biogenesis. PLoS One 4:e4971.
15. Okamura K and Lai EC. (2008). Endogenous small interfering RNAs in animals. Nat Rev Mol Cell Biol 9:673–678.
16. Harfe BD. (2005). MicroRNAs in vertebrate development. Curr Opin Genet Dev 15:410–415.
17. Soifer HS, Rossi JJ and Sætrom P. (2007). MicroRNAs in disease and potential therapeutic applications. Mol Ther 15:2070–2079.
18. Bartel DP. (2004). MicroRNAs: genomics, biogenesis, mechanism, and function. Cell 116:281–297.
19. Tomari Y and Zamore PD. (2005). Perspective: machines for RNAi. Genes Dev 19:517–529.
20. Huang V, Qin Y, Wang J, Wang X, Place RF, Lin G, Lue TF and Li LC. (2010). RNAa is conserved in mammalian cells. PLoS One 5:e8848.
21. Janowski BA, Younger ST, Hardy DB, Ram R, Huffman KE and Corey DR. (2007). Activating gene expression in mammalian cells with promoter-targeted duplex RNAs. Nat Chem Biol 3:166–173.
22. Li LC, Okino ST, Zhao H, Pookot D, Place RF, Urakami S, Enokida H and Dahiya R. (2006). Small dsRNAs induce transcriptional activation in human cells. Proc Natl Acad Sci (USA) 103:17337–17342.
23. Portnoy V, Huang V, Place RF and Li LC. (2011). Small RNA and transcriptional upregulation. Wiley Interdiscip Rev RNA 2:748–760.
24. Shirane D, Sugao K, Namiki S, Tanabe M, Iino M and Hirose K. (2004). Enzymatic production of RNAi libraries from cDNAs. Nat Genet 36:190–196.
25. Shirane D, Sugao K, Namiki S, Tanabe M, Iino M and Hirose K. (2004). Restriction enzyme-generated siRNA (REGS) vectors and libraries. Nat Genet 36:183–189.
26. Luo B, Heard AD and Lodish HF. (2005). Small interfering RNA production by enzymatic engineering of DNA (SPEED). Proc Natl Acad Sci (USA) 101:5494–5499.
27. Pongratz C, Yazdanpanah B, Kashkar H, Lehmann MJ, Kräusslich HG and Krönke M. (2010). Selection of potent non-toxic inhibitory sequences from a randomized HIV-1 specific lentiviral short hairpin RNA library. PLoS One 5:e13172.
28. Seyhan AA, Vlassov AV, Ilves H, Egry L, Kaspar RL, Kazakov SA and Johnston BH. (2005). Complete, gene-specific siRNA libraries: production and expression in mammalian cells. RNA 11:837–846.
29. Shtutman M, Maliyekkel A, Shao Y, Carmack CS, Baig M, Warholic N, Cole K, Broude EV, Harkins TT, Ding Y, Roninson IB. (2010). Function-based gene identification using enzymatically generated normalized shRNA library and massive parallel sequencing. Proc Natl Acad Sci (USA) 107:7377–7382.
30. Xu J, Zeng JQ, Wan G, Hu GB, Yan H and Ma LX. (2009). Construction of siRNA/miRNA expression vectors based on a one-step PCR process. BMC Biotechnol 9:53.
31. Du C, Ge B, Liu Z, Fu K, Chan WC and McKeithan TW. (2006). PCR-based generation of shRNA libraries from cDNAs. BMC Biotechnol 6:28.
32. Tucholski J, Skowron PM and Podhajska AJ. (1995). MmeI, a class-IIS restriction endonuclease: purification and characterization. Gene 157:87–92.
33. Campbell VW and Jackson DA. (1980). The effect of divalent cations on the mode of action of DNase I. The initial reaction products produced from covalently closed circular DNA. J Biol Chem 255:3726–3735.
34. Möncke-Buchner E, Mackeldanz P, Krüger DH and Reuter M. (2004). Overexpression and affinity chromatography

purification of the Type III restriction endonuclease EcoP15I for use in transcriptome analysis. J Biotechnol 114:99–106.
35. Tabor S, Struhl K, Scharf SJ and Gelfand DH. (2001). DNA-dependent DNA polymerases. Curr Protoc Mol Biol Chapter 3:Unit3.5.
36. Livak KJ and Schmittgen TD. (2001). Analysis of relative gene expression data using real-time quantitative PCR and the 2(-delta delta C(T)) method. Methods 25:402–408.
37. Filhol O, Ciais D, Lajaunie C, Charbonnier P, Foveau N, Vert JP and Vandenbrouck Y. (2012). DSIR: assessing the design of highly potent siRNA by testing a set of cancer-relevant target genes. PLoS One 7:e48057.
38. MacRae IJ, Ma E, Zhou M, Robinson CV and Doudna JA. (2008). In vitro reconstitution of the human RISC-loading complex. Proc Natl Acad Sci (USA) 105:512–517.
39. Noland CL, Ma E and Doudna JA. (2011). siRNA repositioning for guide strand selection by human dicer complexes. Mol Cell 43:110–121.
40. Singer O, Yanai A and Verma IM. (2004). Silence of the genes. Proc Natl Acad Sci (USA) 101:5313–5314.
41. Tomimoto K, Yamakawa M and Tanaka H. (2012). Construction of a long hairpin RNA expression library using Cre recombinase. J Biotechnol 160:129–139.
42. Gong W, Ren Y, Zhou H, Wang Y, Kang S and Li T. (2008). siDRM: an effective and generally applicable online siRNA design tool. Bioinformatics 24:2405–2406.
43. Naito Y, Yoshimura J, Morishita S and Ui-Tei K. (2009). siDirect 2.0: updated software for designing functional siRNA with reduced seed-dependent off-target effect. BMC Bioinformatics 10:392.

Address correspondence to:
York Yuanyuan Zhu, PhD
Small RNA Technology and Application Institute
Nantong University
76 Changxing Road
E & T Development Area
Nantong, 226016
China

E-mail: yzhu@biomics.cn

Received for publication October 14, 2014; accepted after revision November 6, 2014.

IVYSPRING INTERNATIONAL PUBLISHER

Journal of Cancer

2016; 7(10): 1317-1327. doi: 10.7150/jca.15157

Research Paper

Multi-target siRNA: Therapeutic Strategy for Hepatocellular Carcinoma

Tiejun Li[1,2,3], Yuwen Xue[1], Guilan Wang[1], Tingting Gu[1], Yunlong Li[1], York Yuanyuan Zhu[2,3]✉, Li Chen[1]✉

1. Department of Pathological Anatomy, Nantong University, Nantong, China;
2. Small RNA Technology and Application Institute, Nantong University, Nantong, China;
3. Biomics Biotechnologies Co., Ltd., Nantong, China.

✉ Corresponding authors: Li Chen, Professor. Department of Pathological Anatomy, Nantong University, 19 Qixiu Road, Nantong 226001, Jiangsu, China. Email: bl1@ntu.edu.cn. York Yuanyuan Zhu, Ph.D. Small RNA Technology and Application Institute, Nantong University, 76 Changxing Road, E&T Development Area, Nantong 226016, China. Email: yzhu@biomics.com. Tel: +86-513-85051729; Fax: +86-513-85051729.

Received: 2016.02.01; Accepted: 2016.05.18; Published: 2016.06.25

Abstract

Multiple targets RNAi strategy is a preferred way to treat multigenic diseases, especially cancers. In the study, multi-target siRNAs were designed to inhibit NET-1, EMS1 and VEGF genes in hepatocellular carcinoma (HCC) cells. And multi-target siRNAs showed better silencing effects on NET-1, EMS1 and VEGF, compared with single target siRNA. Moreover, multi-target siRNA showed greater suppression effects on proliferation, migration, invasion, angiogenesis and induced apoptosis in HCC cells. The results suggested that multi-target siRNA might be a preferred strategy for cancer therapy and NET-1, EMS1 and VEGF could be effective targets for HCC treatments.

Key words: multi-target siRNA, hepatocellular carcinoma (HCC), NET-1, EMS1, VEGF.

Introduction

RNA interference (RNAi) has become a popular approach recently, RNAi technology is applied for posttranscriptional gene silencing which triggered by small interfering RNA (siRNA) [1-3]. RNAi therapies have rapidly been advanced in clinical trials for the treatment of various human diseases, especially various human cancers [4-6], and the strategy of multiple gene-targeted siRNAs is considered to be a good way for controlling complex disease systems [7,8], such as hepatocellular carcinoma (HCC) [9].

HCC is the sixth most common malignancy tumor in the world and HCC has several complex and genetic alterations [10]. But the mechanisms of initiation and progression of HCC have not been made clear completely. Even though there are potential curative treatments, HCC can also easily become a poor prognosis tumor with the characteristics of high recurrence rate and rapid progress [11]. Therefore, development and identification of novel effective agents, such as siRNAs, that are able to suppress HCC effectively is imperative.

NET-1 gene is a member of the transmembrane 4 superfamily (TM4SF) [12], it is a tumor-related gene and found to be high expressed in many human tumor tissues [13-17]. NET-1 overexpression was also strong-related to pathological grading and clinical stages in HCC [18]. EMS1 is a cytoskeleton reorganization related gene, its coding protein is cortical actin-binding protein (cortactin) with binding ability to F-actin [19]. Studies found that cortactin could bind to Arp2/3, and influence cell motility, it also was considered has a relationship with cell migration [18]. Cortactin is a substrate of oncogene *src*, so its functions in tumors are studied deeply, and EMS1 was found high expressed in hepatocarcinoma, breast cancer and head and neck cancer, it had relationship with cancer invasion and transfer [20-23]. Vascular endothelial growth factor (VEGF) is a well-known gene in cancer therapy researches, angiogenesis inhibition is considered as an effective

way for tumor treatment, thus VEGF is a good target for cancer therapy [24-26].

In the study, we intended to evaluate the effects of multiple targeting of NET-1, EMS1 and VEGF genes on biological behavior of HCC cell *in-vitro*.

Materials and Methods

Cell Lines and Cell Culture

Human embryonic kidney cells (HEK293), human HCC cells (MHCC97H, MHCC97L, HepG2, SMMC-7721) and human normal liver cells (LO2) were cultured in Dulbecco's Modified Eagle Medium (DMEM, Gibco) supplemented with 10 % fetal bovine serum (FBS, Gibco), 2 mM L-glutamine, 100 U/ml of penicillin and 100 μg/ml of streptomycin. These cell lines were purchased from the Institute of Cell Biology, Chinese Academy of Sciences, and cells were maintained at 37 °C in a humidified incubator with 5 % CO_2.

Multi-target siRNA Design and siRNA Transfection

The sequence of NET-1 (Accssion No. NM 005727.3), EMS1 (Accssion No. NM 053056) and VEGF (Accssion No. NM 001287044.1) were obtained from National Center of Biotechnology Information (NCBI) GenBank (USA), and the single target siRNAs which targeting either NET-1, EMS1 or VEGF (NET-1_siR, EMS1_siR and VEGF_siR, 19 bp duplex with 2-nt 3'-overhangs) were designed and screened by our precious studies [27, 28]. And a siRNA which sequence has no homology with human genes was designed as negative control (NC_siR). All RNA oligonucleotides were chemically synthesized by Biomics Biotechnologies Co., Ltd. (Biomics Biotech, China). The oligonucleotide sequences were shown in Table 1. The cells were transfected *in-vitro* with siRNAs using Lipofectamine® 2000 transfection reagent (ThermoFisher, USA) according to the manufactures' instructions.

Multi-target siRNAs Design and Synthesis

The multi-target siRNA (mtg_siRs) constructs targeting NET-1, EMS1 and VEGF were designed according to the principle of Biomics Biotech (China) (sequences shown in Table 2). The long single stranded RNAs (the length was >21 nt) were synthesized by *in vitro* transcription mediated by T7 RNA polymerase. Briefly, T7 RNA polymerase promoter (5'-CACTAATACGACTCACTATAGGG-3') conjugated DNA oligos that complementary to the interest RNAs were chemically synthesized. The RNAs were synthesized by T7 RNA polymerase with the rNTPs at 37 °C for 5 h. Final RNA products were obtained post purification.

Table 1. Sequences of the single target siRNAs.

siRNAs	Sequences (5'-3')
NET-1_siR	Sense: CCACAAUGGCUGAGCACUUdTdT
	Antisense: AAGUGCUCAGCCAUUGUGGdTdT
EMS1_siR	Sense: GAACAAGACCGAAUGGAUAdTdT
	Antisense: UAUCCAUUCGGUCUUGUUCdTdT
VEGF_siR	Sense: GGAGUACCCUGAUGAGAUCdTdT
	Antisense: GAUCUCAUCAGGGUACUCCdTdT
NC_siR	Sense: UUCUCCGAACGUGUCACGUdTdT
	Antisense: ACGUGACACGUUCGGAGAAdTdT

Table 2. Sequences of the Multi-target siRNAs (Mtg_siRNA)

Mtg_siRNA	Targets	Sequences (5'-3')
NEV Str1	NET-1	S:CCACAAUGGCUGAGCACUUGGAACAAGACCGA
	EMS1	AUGGAUACGGAGUACCCUGAUGAGAUCdTdT
	VEGF	As1:AAGUGCUCAGCCAUUGUGGdTdT
		As2:UAUCCAUUCGGUCUUGUUCdTdT
		As3:GAUCUCAUCAGGGUACUCCdTdT
NEV Str2	NET-1	S:CCACAAUGGCUGAGCACUUGGAACAAGACCGA
	EMS1	AUGGAUACGGAGUACCCUGAUGAGAUCdTdT
	VEGF	As1:GAUCUCAUCAGGGUACUCCdTdT
		As2:UAUCCAUUCGGUCUUGUUCUUCAAGAGAAAG UGCUCAGCCAUUGUGGdTdT
NEV Str3	NET-1	S:CCACAAUGGCUGAGCACUUGGAACAAGACCGA
	EMS1	AUGGAUACGGAGUACCCUGAUGAGAUCdTdT
	VEGF	As1:AAGUGCUCAGCCAUUGUGGdTdT
		As2:GAUCUCAUCAGGGUACUCCUUCAAGAGAUAU CCAUUCGGUCUUGUUCdTdT

S, Sense Strand; As, Antisense Strand.

Dual Luciferase Reporter Assay

The siRNA validation vector siQuant (kindly provided by Dr. Quan Du of Peking University) [29] was used for detection of the gene silencing activity of mtg_siRs. When the siRNA validation vectors (siQNET-1, siQEMS1 and siQVEGF) were constructed, the activities of mtg_siRs were analyzed by dual luciferase reporter (DLR) assay according to the protocol of Du Q et al. [30]. Briefly, the DNA oligonucleotides were designed (Table 3), synthesized (Biomics Biotech, China) and annealed to DNA duplex. Then they were ligated to construct siRNA validation vectors containing siRNA target site of NET-1, EMS1 or VEGF, and all constructs were verified by sequencing. HEK293 cells were grown and seeded into 24-well plates at 1×10^5 cells/well for 24 h before transfection. The validation vector was co-transfected with pRL-TK (Promega, USA) with or without siRNAs. The cells were harvested after 24 h, according to the DLR assay manual (Promega, USA). And the activities of luciferase were measured on a Luminometer (Promega, USA). The firefly luciferase signal was normalized to the renilla luciferase signal for each individual well, and the knockdown efficacy of each siRNA was evaluated by relative luciferase activity unit (RLU). All experiments were performed in triplicates and repeated three times.

Table 3. Sequences of the siQuant inserts.

siQuant Reporter	Sequences (5′-3′)
siQNET-1	S: GATCTCACCACAATGGCTGAGCACTTCCGGGCC
	As: CGGAAGTGCTCAGCCATTGTGGTGA
siQEMS1	S: ATCTCAAGAACAAGACCGAATGGATACGGGCC
	As: CGTATCCATTCGGTCTTGTTCTTGA
siQVEGF	S: GATCTCAAAGGAGTACCCTGATGAGATCGGGCC
	As: CGATCTCATCAGGGTACTCCTTTGA

S, Sense Strand; As, Antisense Strand.

Real-time Quantity PCR (RT-qPCR)

Total RNA of cells were extracted by RISO™ RNA extraction reagent (Biomics Biotech, China) and then performed to a 25 μL PCR reaction: 12.5 μL of 2×Master Mix (Biomics Biotech, China), 0.5 μL of each forward and reverse primers (10 μM each), 0.5 μL of 50×SYBR Green I and 4 μL total RNA, then subjected to reverse transcription for 30 min at 42 °C and initially denatured at 95 °C for 5 min, and then to 45 cycles of amplification with the condition of: 95 °C denature for 20 s, 55 °C annealing for 30 s, and 72 °C extension for 30 s. Human glyceraldehyde-3-phosphate dehydrogenase (GAPDH) served as an internal control. All primers sequences were shown in Table 4. The experiment was performed in triplicate. The results were analyzed by $2^{-\Delta\Delta Ct}$ method [31].

Table 4. Sequences of RT-qPCR primers.

Gene Name		Sequence (5′-3′)
NET-1	Forward	CTTCATCCTCCTCCTCATCTTC
	Reverse	CAGGCACTACCAGCAACG
EMS1	Forward	AGAGGCTGTCTATGAAAG
	Reverse	GATGTTGGTGATGATGTC
VEGF	Forward	GACATCTTCCAGGAGTACC
	Reverse	TGCTGTAGGAAGCTCATCTC
Cyclin D1	Forward	ATCTACACCGACAACTCCATC
	Reverse	TGTTCTCCTCCGCCTCTG
bFGF	Forward	AGCAGCATCTGTAAGGTTCTTC
	Reverse	TGAAACATTGGGAGGGAAAC
Fascin	Forward	GCTGGAGTTCAACGATGG
	Reverse	ACCTTGTTATAGTCGCAGAAC
OAS1	Forward	GTGAGCTCCTGGATTCTGCT
	Reverse	TGTTCCAATGTAACCATATTTCTGA
IFIT1	Forward	AATAGACTGTGAGGAAGGATGG
	Reverse	TCCAGGCGATAGGCAGAG
GAPDH	Forward	GAAGGTGAAGGTCGGAGTC
	Reverse	GAAGATGGTGATGGGATTTC

Western Blot

1×10^6 cells/well were plated in a 6-well plate and grown for 24 h until about 70% confluence. After cells were treated by siRNAs for 48 h, they were harvested and lysed in RIPA buffer (Pierce, USA). Total protein was separated by polyacrylamide gel electrophoresis (PAGE) and electroblotted onto polyvinylidine difluoride filter (PVDF) membranes (Millipore, USA), followed by blocking with 5% skim milk in TBST (20 mM Tris, 150 mM NaCl, 0.05% Tween-20, pH7.5) buffer for 2 h at room temperature, then incubated with rabbit-anti-human NET-1 antibody (1:500 dilution, Abgent, USA), rabbit-anti-human EMS1 (1:500 dilution, Abcam, USA) and rabbit-anti-human VEGF antibody (1:500 dilution, Abcam, USA), mouse-anti-human β-actin antibody (1:500 dilution, Abcam, USA) as internal control. Then membranes were washed in TBST and incubated with a goat anti-rabbit or goat anti-mouse HRP-conjugated secondary antibody (1:1000 dilution, Jackson, USA) at room temperature for 2 h. At last, the specific proteins were detected with ECL chemiluminescence reagent (Beyotime, China); the membranes were exposed to films (Kodak, USA).

Immunocytochemistry (ICC)

7.5×10^4 cells were cultured on a small round slide in a 24-well plate, when cells grown to about 50% confluence, they were treated as described above. Then cells were fixed with 4% paraformaldehyde for 30 min and permeabilized with 0.5 % Triton X-100 for 10 min, after being washed by PBS, blocked with 1% bovine serum albumin (BSA) for 30 min. Subsequently, cells were incubated at 4 °C overnight with antibodies as used in Western blot, and then with TRITC-conjugated goat-anti-rabbit IgG (for NET-1 or VEGF) and FITC-conjugated goat-anti-rabbit IgG (for EMS1) (1:50 dilution, Boster, China) for 2 h at room temperature. Hoechst 33258 (10 mg/mL) (ThermoFhisher, USA) was used for cell nuclei staining, after washed by PBS and mounted by Antifade Mounting Medium (Beyotime, China), cells were observed under immunofluorescence microscopy.

Cell Viability Assay

The viability of cells was measured by MTT assay. 5×10^3 cells/well were plated into a 96-well plate for 24 h, then treated by siRNAs for 0, 24, 48, 72 and 96 h, 10 μL MTT solution (Beyotime, China) were added to each well of 96-well plate containing 100 μL DMEM and incubated at 37 °C for 4 h, following 150 μL DMSO per well were added and continuing incubated at 37 °C for 10 min. The optical density (OD) was measured at 490 nm using a Microplate Reader (BioRad, USA).

Cell Invasion Assay

2×10^4 cells/well were seeded into a 24-well plate for 24 h and treated as described above for 48 h, then cells were suspended in DMEM at the density of 1×10^6 cells/mL. Briefly, transwell chambers (Corning, USA) were treated with DMEM for 1 h before treatments; the upper and lower chambers were separated by an 8 μm pore polycarbonate membrane which was coated

with 50 μL of 0.5 mg/ml matrigel (BD, USA). 100 μL cell suspension was added into each upper chamber with 600 μL DMEM containing 10% FBS or conditioned medium which were the cell supernatant with siRNAs to perform post-transfection for 48 h. The cells on the top surface of the membrane were carefully removed after 24 h post treatments. Cells on the transwell chambers were fixed for 30 s in 10% formaldehyde, and then stained by 0.5% crystal violet. After being washed by PBS, the cells on the top surface of the membrane were carefully removed again. The cells on the bottom surface of the membrane were counted in 3-5 random fields under microscope (magnification 100×).

Cell Apoptosis Assay

Annexin V-FITC/PI double staining and flow cytometry (FCM) analysis method was used to determine the cell apoptosis. Briefly, 1×10^6 cells/well in a 6-well plate treated with siRNAs for 48 h were harvested and washed in PBS, then re-suspended in binding buffer, followed by incubation with Annexin V-FITC conjugate and PI for 15 min, then detected by FCM analysis (BD Biosciences, USA).

Tube Formation Assay

HUVECs *in-vitro* angiogenesis model was used to evaluate inhibition effect. Briefly, 1×10^5 HUVECs were re-suspended in conditioned medium (which was the supernatant of cells treated with siRNAs for 48 h), then seeded in a 48-well plate which were coated by matrigel (BD, USA), and cultured in at 37 °C/5% CO_2 incubator for 24 h, the numbers of branching points were counted under microscope (magnification 40×).

Cell Migration Assay

Wound-healing assay was used to detect the migration inhibition effect. Briefly, 3×10^5 cells/well were plated and treated as described above in a 12-well plate. Wound was made through confluent monolayer cells with a pipette tip post-transfected for 48 h and cells were washed with DMEM twice. Cell photos were taken at 0, 24, 48, and 72 h to monitor cell migration.

Statistical Analysis

All experiments were performed independently three times, the results were shown as mean ± standard deviation (SD), and statistical analyses were performed using SPSS19.0 software. The differences between two groups were compared using Student's *t-test* and multiple comparisons using one-way ANOVA analysis to assess statistical significance. All *P* values were based on a two-sided statistical analysis and $P<0.05$ was considered to indicate statistical significance.

Results

Multi-target siRNAs were designed and synthesized by chemical and *in vitro* transcription method.

The multi-target siRNAs (mtg_siRs) targeting NET-1, EMS1 and VEGF were designed according to different structures (Fig. 1). The short single stranded RNAs and long single stranded RNAs (the length was >21 nt) of mtg_siRs were synthesized by chemical and *in vitro* transcription method separately, and mtg_siRs were obtained by annealing long RNA and corresponding short RNAs (Table 2, Fig. 1).

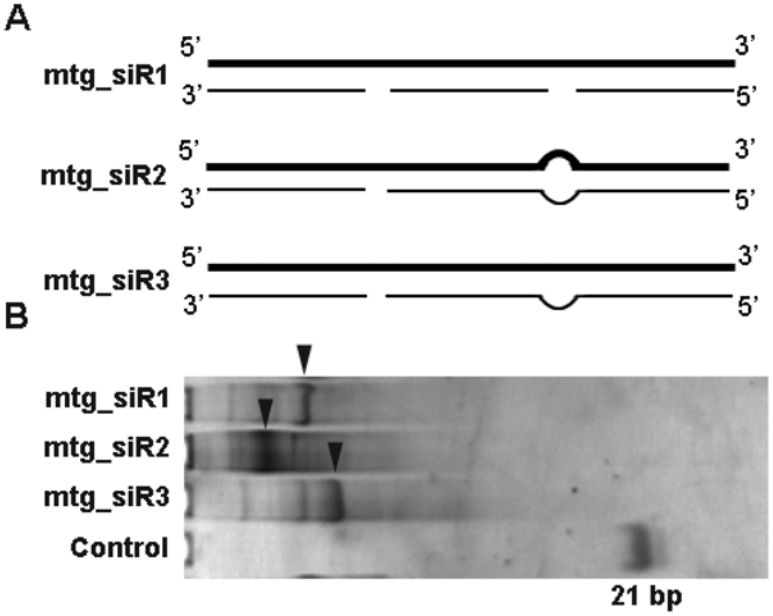

Figure 1. mtg_siRs were designed and synthesized by chemical and *in vitro* transcription method. (A) The designed different mtg_siRs structures, bold lines are sense strands and the thin lines are antisense strands, (B) The synthesitcal mtg_siRs detected by 15% polyacrylamide gelelectrophoresis (PAGE).

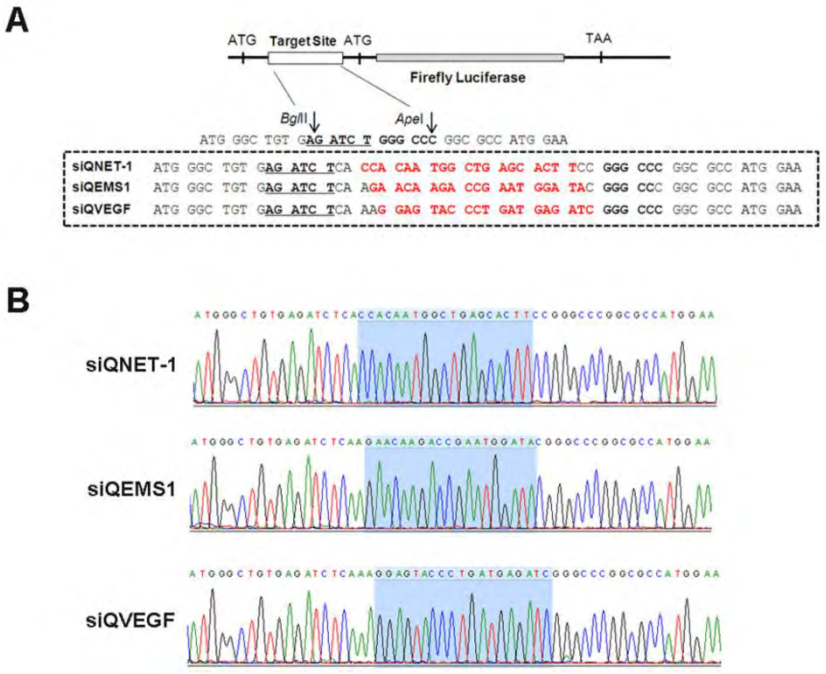

Figure 2. The designed mtg_siRs validation vectors of siQuant method. (A) The designed siRNA target (NET-1, EMS1 and VEGF) siQuant vectors, (B) The sequencing results of different siRNA validation vectors (siQNET-1, siQEMS1 and siQVEGF).

The activities of different multi-target siRNAs detected by DLR assay

The siRNA validation vectors and mtg_siRs were co-transfected into HEK293 cells, and the activities detected by DLR system (Promega, USA). As shown in Fig. 2 and 3, the siRNA validation vectors (siQNET-1, siQEMS1 and siQVEGF) were constructed successfully and the activities of mtg_siRs were indicated by RLU values with different treatments. Compared with control (CTL) and NC_siR, NET-1 inhibition rates of mtg_siR1, mtg_siR2 and mtg_siR3 were 60.95%, 57.49% and 81.13% (P<0.05), EMS1 inhibition rates of mtg_siR1, mtg_siR2 and mtg_siR3 were 70.61%, 62.32% and 64.44% (P<0.05), VEGF inhibition rates of mtg_siR1, mtg_siR2 and mtg_siR3 were 82.91%, 86.73% and 77.76% (P<0.05). The specific gene knockdown could be interfered by interferon (IFN) response induced by long stranded dsRNA [32], thus the expression of OAS1 and IFIT1 genes were used to monitor the IFN response induced by mtg_siRs. 10 ng/mL Poly(I:C) [33] transfection served as positive control. Results showed no obvious IFN response induced by mtg_siRs, compared with positive or negative control (Fig. 3D).

Gene inhibition effects in HCC cell by multi-target siRNAs

The result of RT-qPCR showed that, compared with normal hepatocyte LO2, the mRNA level of NET-1, EMS1 and VEGF were all high expressed in HCC cells (MHCC97H, MHCC97L, HepG2 and SMMC-7721) (P<0.05), especially in SMMC-7721, NET-1 was 7.31-fold, EMS1 was 4.61-fold and VEGF was 7.67-fold higher than in LO2 cell (P<0.05, Fig. 4A), SMMC-7721 cell was chosen to further study.

As shown in Fig. 4B-D, compared to untreated group, NET-1 mRNA was inhibited by NET-1_siR, mtg_siR1, mtg_siR2 and mtg_siR3 up to 27%, 31%, 25% and 33% (P<0.05). EMS1 was inhibited by EMS1_siR, mtg_siR1, mtg_siR2 and mtg_siR3 up to 28%, 14%, 37% and 24% (P<0.05). VEGF was inhibited by VEGF_siR, mtg_siR1, mtg_siR2 and mtg_siR3 up to 29%, 18%, 17% and 19% (P<0.05), and there was no difference among mtg_siR1, mtg_siR2 and mtg_siR3 and there was no difference between NC_siR and untreated group (P>0.05).

As shown in Fig. 5, the results of Western blot showed that, compared to untreated group, NET-1 protein level was inhibited by mtg_siR1, NET-1_siR, EMS1_siR and VEGF_siR up to 54%, 58%, 70% and 84% (P<0.05). EMS1 was inhibited by mtg_siR1, NET-1_siR, EMS1_siR and VEGF_siR up to 47%, 73%, 45% and 67% (P<0.05). VEGF was inhibited by mtg_siR1, NET-1_siR, EMS1_siR and VEGF_siR up to 39%, 69%, 71% and 48% (P<0.05), and there was no difference between NC_siR and untreated group (P>0.05).

The inhibition effects on the protein level of target genes were further determined by ICC method. As show in Fig. 6, the protein of NET and VEGF were labeled by TRITC (red), and EMS1 was labeled by

FITC (green), the cell nuclei stained by Hoechst (blue). The results showed that the expression of NET-1, EMS1 and VEGF were inhibited by mtg_siR1, compared to NC_siR and untreated group.

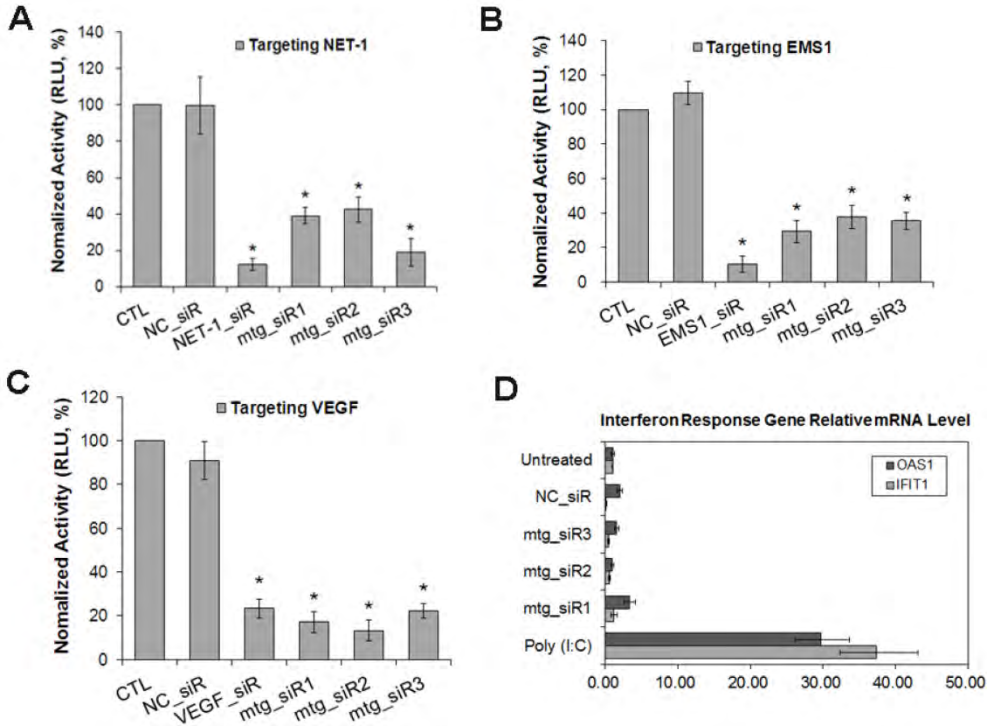

Figure 3. The inhibition activities of mtg_siRs validated by DLR assay. (A) siQNET-1 inhibited by mtg_siRs, (B) siQEMS1 inhibited by mtg_siRs, (C) siQVEGF inhibited by mtg_siRs, *P<0.05, (D) No interferon response induced by mtg_siRs.

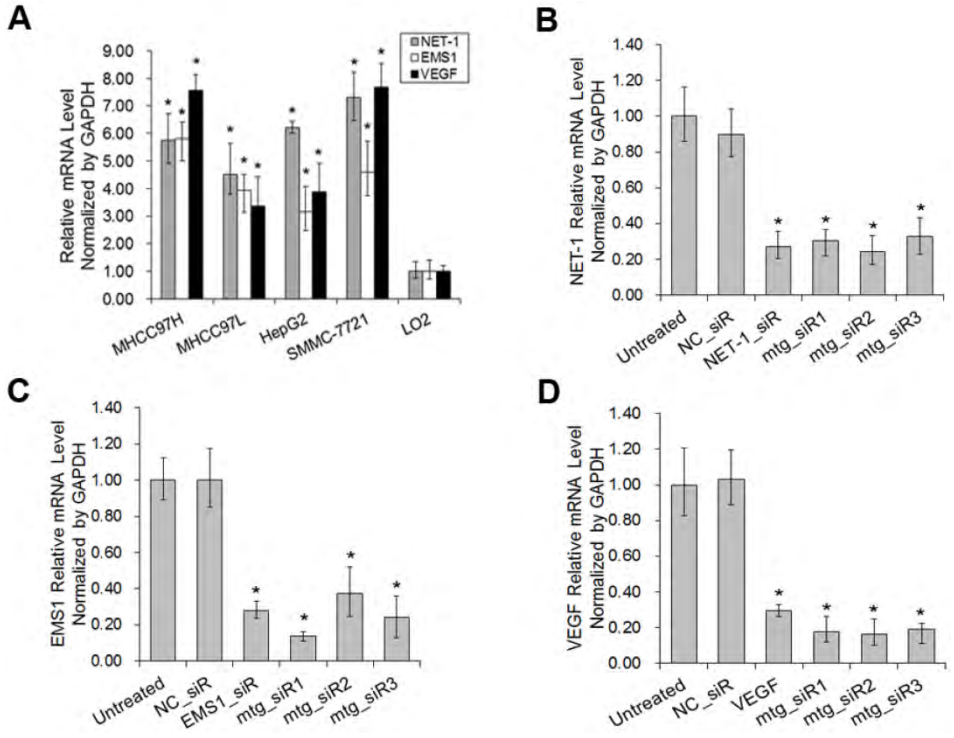

Figure 4. The mRNA expression level of NET-1, EMS1 and VEGF in HCC cells detected by RT-qPCR. (A) The mRNA expression level of NET-1, EMS1 and VEGF in different HCC cells, *P<0.05 vs LO2, (B) The expression of NET-1 inhibited by mtg_siRs in mRNA level, (C) The expression of EMS1 inhibited by mtg_siRs in mRNA level, (D) The expression of VEGF inhibited by mtg_siRs in mRNA level. *P<0.05 vs untreated group.

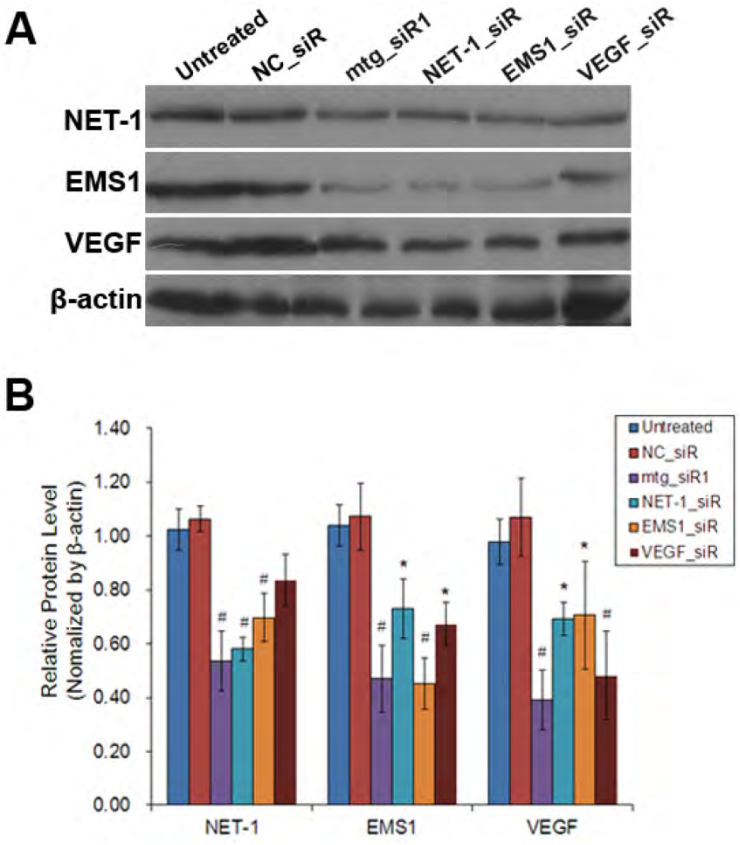

Figure 5. The inhibition of NET-1, EMS1 and VEGF in protein level. (A) The inhibition of NET-1, EMS1 and VEGF in protein level measured by Western blot, (B) The inhibition rate of different treatments, *P<0.05 vs untreated group.

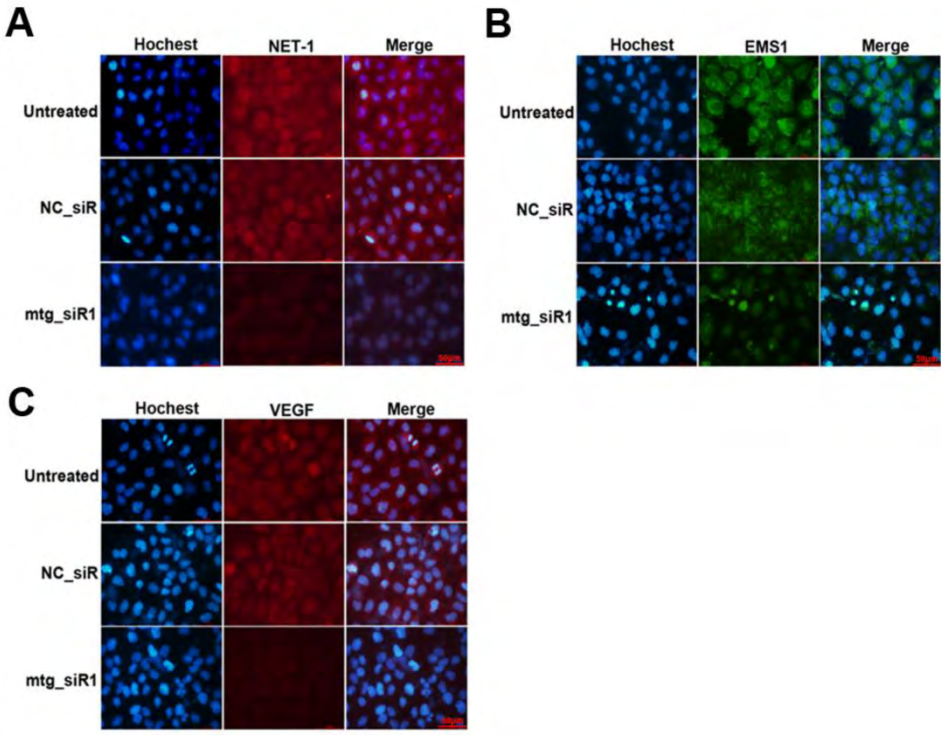

Figure 6. Inhibition effects of target gene by multi-target siRNA in HCC cell measured by ICC. (A) The expression of NET-1 inhibited by mtg_siR1, (B) The expression of EMS1 inhibited by mtg_siR1, (C) The expression of VEGF inhibited by mtg_siR1.

Proliferation and apoptosis relative genes regulated by multi-target siRNA

The mRNA expression levels of Cyclin D1, Fascin and bFGF were determined by RT-qPCR post siRNA treatments. The expression of Cyclin D1, Fascin and bFGF were all down-regulated on different level (P<0.05) by mtg_siR1 and corresponding single target siRNA (Fig. 7), compared with NC_siR and untreated group.

Inhibition effect of cell viability by multi-target siRNA

The viability of SMMC-7721 cells was measured by MTT assay. The absorbance values (490 nm) of the cells at 48, 72 and 96 h post-transfection with mtg_siR1, NET-1_siR, EMS1_siR and VEGF_siR were significantly lower than those of NC_siR treated cells and untreated cells respectively. There was no significant difference between the growth of cells treated with NET-1_siR, EMS1_siR and VEGF_siR, and the cell viability in mtg_siR1 treated group showed a significant decrease (P<0.05, Fig. 8A).

Inhibition effect of cell invasion by multi-target siRNA

The cell invasion abilities with different treatments were detected by transwell assay, as Fig. 8B showed that the invasion of the cells treated with mtg_siR1, NET-1_siR, EMS1_siR and VEGF_siR were inhibited significantly post 48 h transfection (P<0.05). There was no significant difference of inhibition abilities between NC_siR and untreated cells (P>0.05), and the number of invasion cells in mtg_siR1 treated group was significantly decreased than that of NET-1_siR, EMS1_siR and VEGF_siR (P<0.05).

Cell apoptosis induced by multi-target siRNA

Annexin V-FITC/PI double staining and FCM analysis were used to detect the ability of mtg_siR on inducing SMMC-7721 cell apoptosis. As shown in Fig. 8C, treatments with mtg_siR1 (28.93±1.93), NET-1_siR (15.46±1.47%), EMS1_siR (10.64±2.91), and VEGF_siR (15.82±1.40) resulted in a significant increase of apoptosis compared with that of NC_siR treated cells (3.08±0.97%) and untreated cells (2.40±0.54%) (P<0.05), and the apoptosis rate of mtg_siR1 treated group were higher than that of NET-1_siR, EMS1_siR and VEGF_siR (P<0.05).

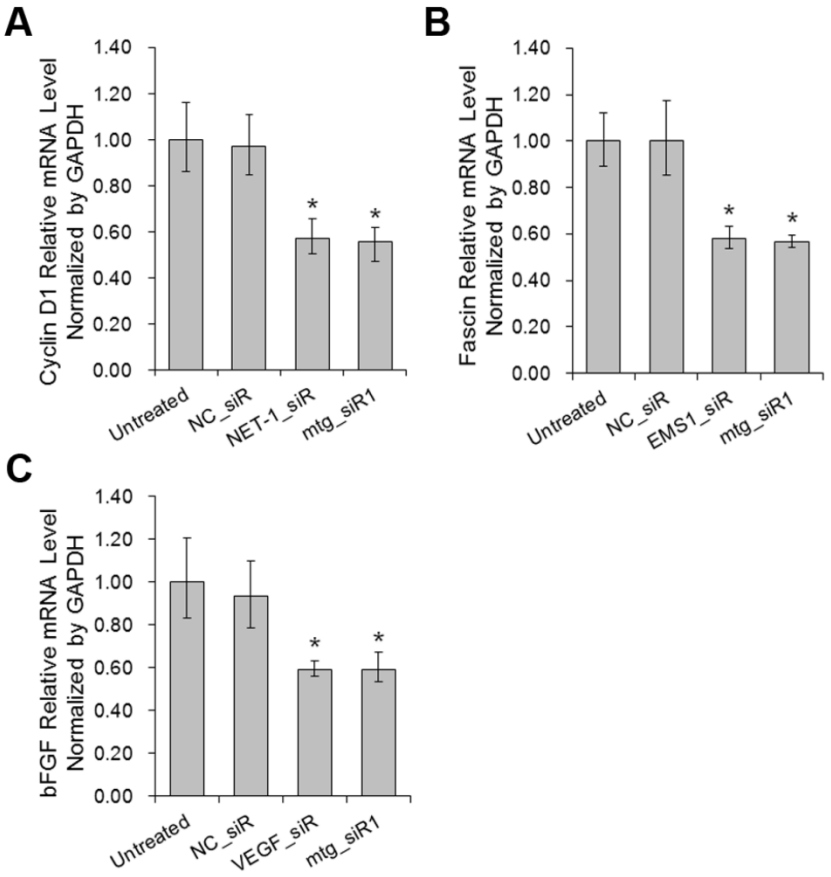

Figure 7. The affection of proliferation and apoptosis relative genes when down-regulation of NET-1, EMS1 and VEGF detected by RT-qPCR. (A) The mRNA level of proliferation gene Cyclin D1, (B) The mRNA level of motility gene Fascin, (C) The mRNA level of fibroblast growth factor bFGF, *P<0.05 vs untreated group.

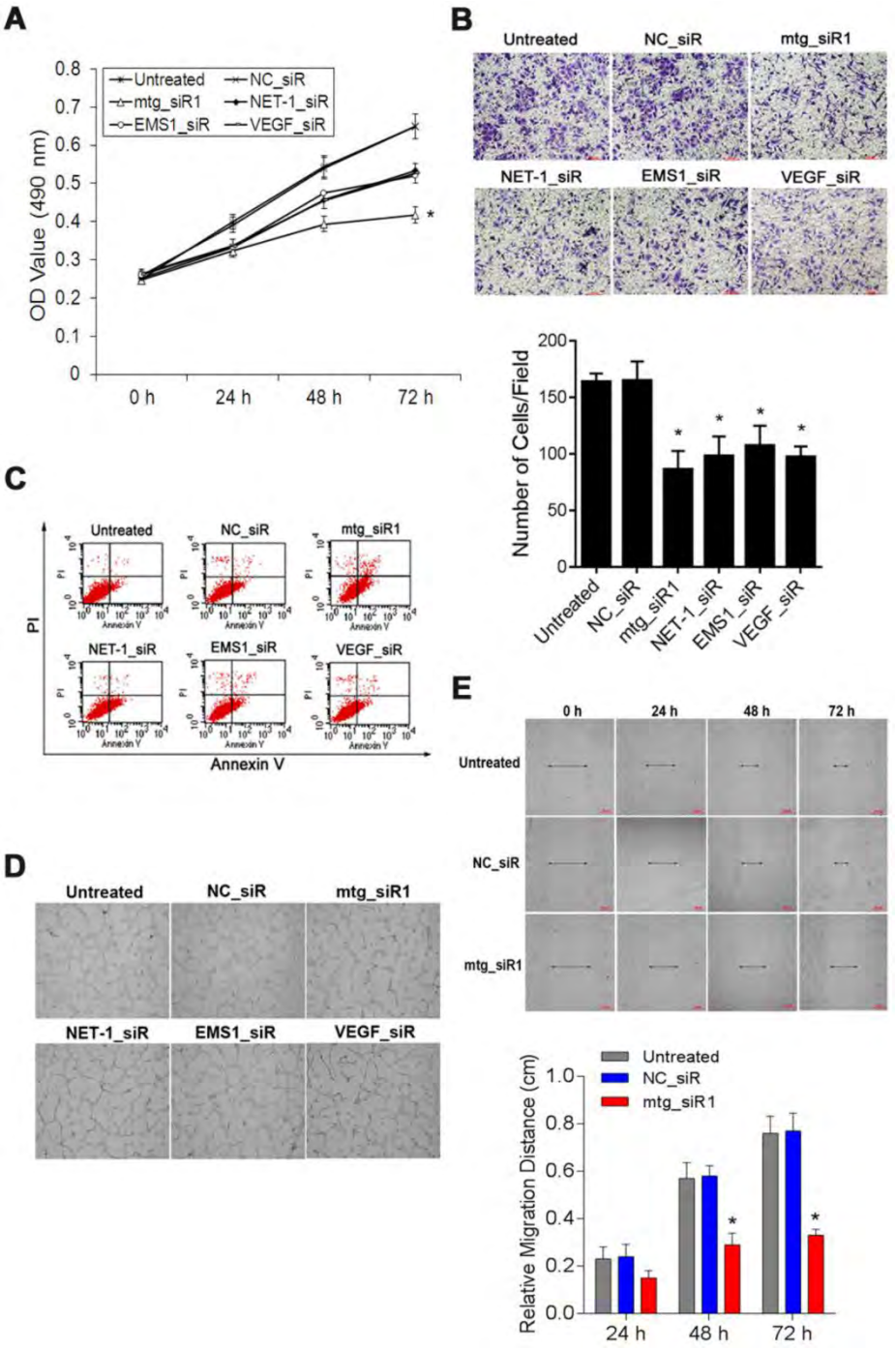

Figure 8. The suppression effects on cell viability, invasion, angiogenesis, migration and induced apoptosis by mtg_siR. (A) Cell growth curve of all groups at 0 h, 24 h, 48 h, 72 h, (B) Representative field photograph of transwell chamber assay under single-target siRNA and mtg_siR treatment after 48 h, (C) Cell apoptosis was measured by FCM analysis after AnnexinV/PI staining, (D) The tube formation photographs of each treatment in HUVECs angiogenesis model, (E) The ability of cell migration at 0 h, 24 h, 48 h, 72 h.

Influence effect of multi-target siRNA on tube formation

The tube formation was evaluated in HUVEC angiogenesis model, HUVECs stimulated by the conditioned medium derived from SMMC-7721 cells transfected with mtg_siR1, NET-1_siR, EMS1_siR and VEGF_siR. As illustrated in Fig. 8D, HUVECs treated with the conditioned medium of mtg_siR1, NET-1_siR, EMS1_siR and VEGF_siR were inhibited to form extensive and enclosed tube networks as compared with the untreated ones. The numbers of branching points were counted that mtg_siR1 (11.00±2.00), NET-1_siR (27.67±1.53), EMS1_siR (27.33±4.51), and VEGF_siR (15.33±2.08) less than NC_siR (69.33±3.06) and untreated cells (72.00±3.61) significantly (P<0.05).

Inhibition effect of cell migration by multi-target siRNA

The migration ability of SMMC-7721 cells inhibited by mtg_siR was measured by wound-healing assay. The scratch caused in groups of untreated and NC_siR nearly closed completely after 72 h, but the cells in treatment with NET-1_siR, EMS1_siR and VEGF_siR were not able to move toward the center of the wound. Compared to the NC_siR treated and untreated cells, the abilities of wound healing in NET-1_siR, EMS1_siR and VEGF_siR treated cells were decreased, and the migration distance in mtg_siR1 treated cells was significantly shorter than that of NET-1_siR, EMS1_siR and VEGF_siR (Fig. 8E).

Discussion

Multi-targeting therapies for cancers have been considered to be an effective approach, and RNAi strategy is a better method for multiple genes suppression, and there are many siRNA drugs in clinical trials which two or more gene inhibition simultaneously [8]. On the other hand, structural modified siRNAs had been widely used in RNAi therapeutics development, especially long double-stranded RNAs (dsRNA) were designed for carrying two or more siRNA sequences which targeting two or more parts in one mRNA or two or more mRNAs [34-36]. Current studies showed that, once long dsRNAs get into mammalian cells, they can be used as Dicer's substrates for siRNAs processing, then the corresponding genes could be inhibited effectively by siRNAs [1,2,8].

In our study, we designed a series of multi-target siRNA structures for triple cancer genes inhibition in hepatocellular carcinoma. We chose NET-1, EMS1 and VEGF as three target genes. NET-1 was reported as a cancer cell proliferation related gene [37], EMS1 was a cancer cell motility and transfer gene [28] and VEGF was angiogenesis related gene in tumor tissues [25]. In our previous studies, we designed and screened better siRNAs that targeting NET-1, EMS1 or VEGF gene respectively [27, 28]. Here, the multi-target siRNAs were designed for carrying on three different siRNA sequences which targeting NET-1, EMS1 and VEGF genes (Table 2, Fig. 1). In detail, three different long dsRNA structures containing three functional siRNA targets, but long RNA chemical synthesis method currently cannot meet our purpose, so the long RNAs were synthesized by T7 polymerase-mediated *in vitro* transcription (as shown in Fig. 1, know-how technology of Biomics Biotechnologies Co., Ltd).

To validate the functions of designed multi-target siRNA structures accurately and quickly, we used a dual luciferase reporter (DLR) assay based on siQuant method [29]. The result showed that three designed structures (mtg_siR1, mtg_siR2 and mtg_siR3) were all have gene silencing efficiencies (Fig. 3). Then, we screened a HCC cell line (SMMC-7721) with high expressed NET-1, EMS1 and VEGF simultaneously for *in-vitro* functional study (Fig. 4). The mRNA and protein levels of NET-1, EMS1 and/or VEGF were suppressed by mtg_siR, NET-1_siR, EMS1_siR and VEGF_siR respectively (Fig. 4-6). And the proliferation gene (Cyclin D1), motility gene (Fascin) and fibroblast growth factor (bFGF) were determined to confirm the inhibition effects of the three genes (Fig. 7).

Furthermore, we demonstrated that the proliferation, migration, invasion and induced apoptosis of HCC cells were inhibited by multi-target siRNA (mtg_siR1) effectively, and the angiogenesis was also suppressed by it (Fig. 8).

The results of the *in-vitro* study were demonstrated that the designed multiple targeting siRNA (mtg_siR1) construct had RNAi activities on knockdown triple genes simultaneously. Moreover, NET-1, EMS1 and VEGF gene silencing simultaneously triggered by siRNA was much better than single target siRNA in the inhibition of either NET-1, EMS1 or VEGF gene. And, co-silencing of NET-1, EMS1 and VEGF could suppress the proliferation, migration, invasion and angiogenesis, while inducing apoptosis of HCC cells *in-vitro*.

The results showed that, multi-target siRNA might be a preferred strategy for multigenic disease therapy for cancers. Also, the result suggested that NET-1, EMS1 and VEGF would be effective target genes for HCC therapy.

Acknowledgments

This study was supported by the foundation of the production-study-research prospective joint research programs of Jiangsu Province, China (No. BY 2013042-06), and a project funded by the Priority Academic Program Development of Jiangsu Higher Education Institutions, and from the Science Foundation of Nantong City, Jiangsu Province, China (nos. BK 2014001 and HS 2014004).

Competing Interests

The authors have declared that no competing interest exists.

References

1. Fire A, Xu S, Montgomery MK, et al. Potent and specific genetic interference by double-stranded RNA in Caenorhabditis elegans. Nature 1998; 391:806-811.
2. Hammond SM, Bernstein E, Beach D, et al. An RNA-directed nuclease mediates post-transcriptional gene silencing in Drosophila cells. Nature 2000; 404:293-296.

3. Elbashir SM, Lendeckel W, Tuschl T. RNA interference is mediated by 21- and 22-nucleotide RNAs. Genes Dev 2001; 15:188-200.
4. Takeshita F, Ochiya T. Therapeutic potential of RNA interference against cancer. Cancer Sci 2006; 97: 689-696.
5. Aigner A. Applications of RNA interference: current state and prospects for siRNA-based strategies in vivo. Appl Microbiol Biotechnol 2007; 76:9-21.
6. Davidson BL, MCCRAY PB. Current prospects for RNA interference-based therapies. Nat Rev Genet 2011; 12:329-340.
7. Zimmermann GR, Leha RJ, Keith CT. Multi-target therapeutics: when the whole is greater than the sum of the parts. Drug Discov Today 2007; 12:34-42.
8. Li T, Wu M, Zhu YY, et al. Development of RNA interference-based therapeutics and application of multi-target small interfering RNAs. Nucleic Acid Ther 2014; 24:302-312.
9. Tabernero J, Shapiro GI, LoRusso PM, et al. First-in-humans trial of an RNA interference therapeutic targeting VEGF and KSP in cancer patients with liver involvement. Cancer Discov 2013; 3:406-417.
10. Forner A, Gilabert M, Bruix J, et al. Treatment of intermediate-stage hepatocellular carcinoma. Nat Rev Clin Oncol 2014; 11:525-535.
11. Bruix J, Gores GJ, Mazzaferro V. Hepatocellular carcinoma: clinical frontiers and perspectives. Gut 2014; 63:844-855.
12. Yauch RL, Hemler ME. Specific interactions among transmembrane 4 superfamily (TM4SF) proteins and phosphoinositide 4-kinase. Biochem J 2000; 35:629-637.
13. Chen L, Wang Z, Zhan X, et al. Association of NET-1 gene expression with human hepatocellular carcinoma. Int J Surg Pathol 2007; 15:346-353.
14. Chen L, Yuan D, Wang GL, et al. Clinicopathological significance of overexpression of TSPAN1, Ki67 and CD34 in gastric carcinoma. Tumori 2008; 94:529-536.
15. Chen L, Zhu YY, Zhang XJ, et al. TSPAN1 protein expression: a significant prognostic indicator for patients with colorectal adenocarcinoma. World J Gastroenterol 2009; 15:2270-2276.
16. Scholz CJ, Kurzeder C, Koretz K, et al. Tspan-1 is a tetraspanin preferentially expressed by mucinous and endometrioid subtypes of human ovarian carcinomas. Cancer Lett 2009; 275:198-203.
17. Zhang J, Wang J, Chen L, et al. Expression and function of NET-1 in human skin squamous cell carcinoma. Arch Dermatol Res 2014; 306:385-397.
18. van Rossum AG, Schuuring-Scholtes E, van Buuren-van Seggelen V, et al. Comparative genome analysis of cortactin and HS1: the significance of the Factin binding repeat domain. BMC Genomics. 2005; 6:15.
19. Chuma M, Sakamoto M, Yasuda J, et al. Overexpression of cortactin is involved in motility and metastasis of hepatocellular carcinoma. J Hepatol. 2004; 41:629-636.
20. Chen L, Wang Z, Zhu J, et al. Roles of cortactin, an actin polymerization mediator, in cell endocytosis. Acta Biochim Biophys Sin (Shanghai). 2006; 38:95-103.
21. Zhu J, Zhou K, Hao JJ, et al. Regulation of Cortactin/Dynamin interaction by actin polymerization during the fission of clathrin-coated pits. J Cell Sci. 2005; 118:807-817.
22. Hao JJ, Zhu J, Zhou K, et al. The coiled-coil domain is required for HS1 to bind to F-actin and activate Arp2/3 complex. J Biol Chem 2005; 280:37988-37994.
23. Lin J, Liu J, Wang Y, et al. Differential regulation of Cortactin and WASP mediated actin polymerization by missing in metastasis (MIM) protein. Oncogene 2005; 24:2059-2066.
24. Yasuda S, Arii S, Mori A, et al. Hexokinase II and VEGF expression in liver tumors: correlation with hypoxia-inducible factor 1 alpha and its significance. J Hepatol 2004; 40:117-123.
25. Rapisarda A, Melillo G. Role of the VEGF/VEGFR axis in cancer biology and therapy. Adv Cancer Res 2012; 114:237-267.
26. Sitohy B, Nagy JA, Dvorak HF. Anti-VEGF/VEGFR therapy for cancer: reassessing the target. Cancer Res 2012; 72:1909-1914.
27. Wu YY, Chen L, Wang GL, et al. Inhibition of hepatocellular carcinoma growth and angiogenesis by dual silencing of NET-1 and VEGF. J Mol Histol 2013; 44:433-445.
28. Zhou J, Chen L, Zhang Y, et al. Synergistic effect of EMS1-shRNA and sorafenib on proliferation, migration, invasion and endocytosis of SMMC-7721. J Mol Histol 2014; 45:205-216.
29. Du Q, Thonberg H, Zhang HY, et al. Validating siRNA using a reporter made from synthetic DNA oligonucleotides. Biochem Biophys Res Commun 2004; 325:243-249.
30. Du Q, Thonberg H, Wang J, et al. A systematic analysis of the silencing effects of an active siRNA at all single-nucleotide mismatched target sites. Nucleic Acids Res 2005; 33:1671-1677.
31. Livak KJ, Schmittgen TD. Analysis of relative gene expression data using real-time quantitative PCR and the 2(-Delta Delta C(T)) Method. Methods 2001; 25:402-408.
32. Elbashir SM, Harborth J, Lendeckel W, et al. Duplexes of 21-nucleotide RNAs mediate RNA interference in cultured mammalian cells. Nature 2001; 411:494-498.
33. Palchetti S, Starace D, De Cesaris P, et al. Transfected poly(I:C) activates different dsRNA receptors, leading to apoptosis or immunoadjuvant response in androgen-independent prostate cancer cells. J Biol Chem 2015; 290:5470-83.
34. Shin D, Lee H, Kim SI, et al. Optimization of linear double-stranded RNA for the production of multiple siRNAs targeting hepatitis C virus. RNA 2009; 15:898-910.
35. Chang CI, Kang HS, Ban C, et al. Dual-target gene silencing by using long, synthetic siRNA duplexes without triggering antiviral responses. Mol Cells 2009; 27:689-695.
36. Rice RR, Muirhead AN, Harrison BT, et al. Simple, robust strategies for generating DNA-directed RNA interference constructs. Methods Enzymol 2005; 392:405-419.
37. Chen L, Li X, Wang GL, et al. Clinicopathological significance of overexpression of TSPAN1, Ki67 and CD34 in gastric carcinoma. Tumori 2008; 94:529-536.